Event-Triggered H_∞ Load Frequency Control for Multiarea Power Systems Under Hybrid Cyber Attacks

Jinliang Liu, Yuanyuan Gu, Lijuan Zha, Yajuan Liu, and Jie Cao

***Abstract*—This paper investigates the problem of event-triggered H_∞ load frequency control (LFC) for multiarea power systems under hybrid cyber attacks, including denial-of-service (DoS) attacks and deception attacks. An event-triggered transmission scheme is developed under the DoS attacks to lighten the load of network bandwidth while preserving a satisfactory system performance. Then, a new switched system model accounting for the simultaneous presence of DoS attacks and stochastic deception attacks is established with respect to the LFC for multiarea power system. On the basis of the new model, sufficient conditions ensuring multiarea power system exponentially mean-square stable with prescribed H_∞ performance are obtained by using Lyapunov stability theory. Furthermore, criteria for simultaneously designing the weighting matrix in event-triggered scheme and the controller gain matrix are derived by utilizing the linear matrix inequality technique. Finally, a three-area power system is simulated to demonstrate the usefulness of the approaches proposed in this paper.**

***Index Terms*—Deception attacks, denial-of-service (DoS) jamming attacks, event-triggered scheme, load frequency control (LFC), network-based power systems.**

I. Introduction

LOAD frequency control (LFC) plays a crucial role in power systems since it is responsible for maintaining the system frequency and the power exchange between areas at desired scheduled values [1]. An important issue on stabilizing LFC power systems is to design suitable control strategies. More recently, a number of notable results on this issue have been reported in the literature. To mention a few, a two-layer active disturbance rejection control approach for LFC of interconnected power system is proposed in [2]. Hanwate *et al.* [3] explored an adaptive policy for LFC to enhance or decrease the activity of two controllers as per their performance throughout the control operation. A new distributed load frequency controller is designed in [4] for smart grids by considering the limited communication resource and speed droop parametric uncertainty. Among all the LFC control design strategies, the most widely used one for industry practice is to adopt a proportional-integral (PI) controller [5]. For instance, the PI-based load frequency controller is applied in [6] for power systems subject to time-varying delays. In [7], the PI controller for LFC power systems is employed once more by considering probabilistic interval delays. It is worth mentioning that due to the urgent need of developing smart grids based on the multiarea power systems, open communication infrastructure is deployed in the feedback loop of a LFC power system, which supports the measurements transmission from a remote telemetry unit to the area controller [4]. In this regard, the LFC power system can be deemed as a representative example of networked control systems (NCSs) [1]. Benefiting from the introduction of open network, the monitoring, dispatch, and scheduling of power systems can be greatly enhanced. At the same time, the problem of network security and the constraint of limited bandwidth are becoming increasing acute.

In the NCS security control literature, a great surge of interest has been witnessed during the past several years since the data transmission medium is prone to be threatened by potential cyber attacks. In the presence of cyber attacks, the data integrity and availability [8] are the common attack targets, which refer to the trustworthiness of data and the ability of a system being accessible, respectively. In accordance with the attack targets, the cyber attacks can be classified into two major types, i.e., deception attack and denial-of-service (DoS) attack. Deception attack corrupts the integrity by replacing the measurable data [9] normally transmitted in the communication channel with fake information. DoS attack corrupts the availability by blocking the transmission medium, which results in the loss of information. Up to date, many researchers have made significant effort in the cyber-security under deception and/or DoS attacks. For example, in [10], the random occurring nature of deception attacks

Manuscript received October 2, 2018; revised November 29, 2018; accepted January 20, 2019. This work was supported in part by the Natural Science Foundation of Jiangsu Province of China under Grant BK20171481, in part by the National Natural Science Foundation of China under Grant 61403185, Grant 61773218, and Grant 61473156, and in part by the Natural Science Foundation of the Jiangsu Higher Education Institutions of China under Grant 18KJB120002. This paper was recommended by Associate Editor Q.-L. Han. *(Corresponding author: Jie Cao.)*

J. Liu is with the College of Information Engineering, Nanjing University of Finance and Economics, Nanjing 210023, China, and also with the College of Automation Electronic Engineering, Qingdao University of Science and Technology, Qingdao 266061, China (e-mail: liujinliang@vip.163.com).

Y. Gu, L. Zha, and J. Cao are with the College of Information Engineering, Nanjing University of Finance and Economics, Nanjing 210023, China (e-mail: guyuanyuan0203@163.com; zhalijuan@vip.163.com; caojie690929@163.com).

Y. Liu is with the School of Control and Computer Engineering, North China Electric Power University, Beijing 102206, China (e-mail: yajuan.liu.12@gmail.com).

Color versions of one or more of the figures in this paper are available online at http://ieeexplore.ieee.org.

Digital Object Identifier 10.1109/TSMC.2019.2895060

is investigated by introducing stochastic variables obeying the given Bernoulli distributions. The remote state estimation over multisensor networks under deception attacks is investigated in [11] and [12]. Befekadu *et al.* [13] addressed the risk-sensitive stochastic control issue under DoS attack, which is modeled as a Markov chain. By considering the effect of energy-limited DoS attacks, a resilient event-triggered H_∞ control approach is proposed in [14] for multiarea power systems. Another kind of energy-limited attack, which is carried out by periodic or pulsewidth-modulated (PWM) signals, are discussed in [16] and [17], when respectively, exploring the resilient event-triggered controller design problem for NCSs and the state estimation issue for cyber-physical systems (CPSs). It should also be pointed out that, up until now, efforts have been bestowed on the malicious cyber attacks against different forms of networked systems, such as neural networks [18], NCSs [19], and CPSs [20], [21]. However, the security problem for LFC multiarea power systems under hybrid cyber attacks has not been fully investigated, which first motivates this paper effort.

In order to mitigate the congested network traffic resulting from the constraint of limited bandwidth, a great number of researchers are dedicated to designing proper transmission strategies to reduce the redundant occupation of communication channel and fruitful results are available in [22]–[30]. Among various transmission strategies, event-triggered transmission scheme represents an effective and efficient one. The core idea of an event-triggered transmission scheme is that not all the periodically sampled measurements but those violating the prescribed transmission-trigger condition will be transmitted over the network. Not surprisingly, a variety of event-triggered transmission schemes have been put forward in the literature. To name only a few, in [31], the transmission event is triggered at the discrete moments when the judgement criterion related to the current sampled data and the error between current sampled data and the last transmitted one is untenable. In order to reduce the burden of network bandwidth under different complex network environment while guaranteeing a desired system performance, some latest results have been derived by improving the event-triggered scheme in [31]. For example, Zhang and Han [32] extended the discrete event-triggered scheme to the dynamic output feedback control problem for NCSs. In [33], a higher energy-efficient mixed sampling scheme is developed by introducing a dynamic adjustable threshold, which can compensate the delay existing in some periodic event-triggered scheme. By taking full advantage of both absolute and relative error-based event-triggered transmission schemes, an integrated sampled-data-based event-triggered communication scheme is presented in [34] when solving the problem of event-triggered consensus for nonlinear multiagent system. For more results on event-triggered transmission schemes, we refer readers to the recent surveys [35]–[39]. It should be pointed out that, although a number of event-triggered control results have been available for various NCSs, seldom attention has been paid to the design of suitable event-triggered transmission schemes when the effects of hybrid cyber attacks are inevitable, especially for the multiarea power system, which serves as the second motivation of this paper.

Based on the observations above, this paper focuses on the issue of event-triggered H_∞ LFC for multiarea power systems under hybrid cyber attacks. The contributions of this paper are threefold.

1) An event-triggered scheme is proposed in the presence of DoS attacks, which are carried out by a class of periodically detectable jammers.
2) By taking the event-triggered scheme under DoS attacks and deception attacks into consideration, a new model for LFC multiarea power system is constructed as a switched system.
3) On the basis of the new model, the exponentially mean-square stability of LFC multiarea power system is obtained by virtue of Lyapunov stability theory.

Furthermore, the weighting matrix in event-triggered scheme and the controller gain are co-designed definitely in terms of the linear matrix inequality (LMI) techniques.

The remainder of this paper is organized as follows. In Section II, problem formulation and preliminaries are outlined and a new switched system model for multiarea power system is established with event-triggered scheme under hybrid cyber attacks. Section III shows the main results concerning the sufficient stabilization conditions for LFC power systems and the H_∞ controller design method. Moreover, both weighting matrix in event-triggered scheme and controller gain are obtained. An illustrative example is given in Section IV to show the usefulness of the design method. The conclusion is presented in Section V.

Notation: $\mathbb{R}$ represents the set of reals and $\mathbb{N}$ represents the set of natural numbers. Given $\nu \in \mathbb{R}$, $\mathbb{R}_{>\nu}$ ($\mathbb{R}_{\geq\nu}$) means the set of reals, which are greater than (greater than or equal to) ν. $\mathbb{R}^n$ denotes the n-dimensional Euclidean space and $\mathbb{R}^{n\times m}$ denotes the set of $n\times m$ real matrices. $\|\cdot\|$ denotes the Euclidean norm. The real symmetric positive definite matrix X is denoted by the notation $X > 0$ for $X \in \mathbb{R}^{n\times n}$. The superscript T indicates matrix transposition. For a symmetric matrix $\begin{bmatrix} A & * \\ B & C \end{bmatrix}$ with $A > 0$ and $C > 0$, $*$ refers to the entries caused by symmetry. $\mathrm{sym}(B)$ represents the symmetrized expression $B + B^{\mathrm{T}}$ for matrix B. I denotes the identity matrix of appropriate dimension. $\mathbb{E}$ is the expectation operator. $\mathcal{L}_2[0,\infty)$ describes the space of square-integrable vector functions over $[0,\infty)$.

II. Problem Formulation

A. System Description

The block diagram for the ith control area in multiarea LFC power systems is shown in Fig. 1, where the signal of area control error (ACE) is assumed to be transmitted to PI controller over an open network.

For the ith-area of LFC power systems, the parameters are listed in Table I and the dynamic model [14] is given as follows:

$$\begin{cases} \dot{\bar{x}}(t) = \bar{A}\bar{x}(t) + \bar{B}u(t) + \bar{E}\omega(t) \\ \bar{y}(t) = \bar{C}\bar{x}(t) \end{cases} \tag{1}$$

where

$$\bar{x}(t) = \begin{bmatrix} \bar{x}_1^{\mathrm{T}} & \dots & \bar{x}_n^{\mathrm{T}} \end{bmatrix}^{\mathrm{T}},\ u(t) = \begin{bmatrix} u_1^{\mathrm{T}} & \dots & u_n^{\mathrm{T}} \end{bmatrix}^{\mathrm{T}}$$

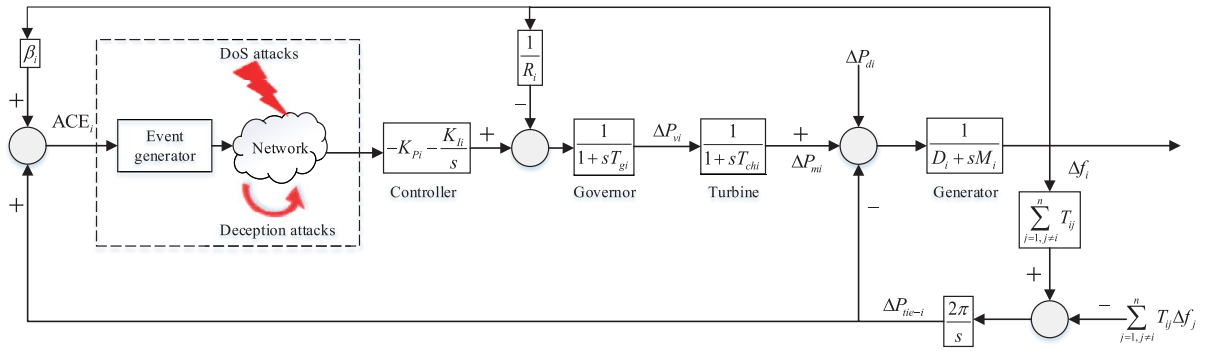

Fig. 1. Dynamic model of the ith LFC power system with event-triggered scheme under hybrid cyber attacks.

TABLE I
PARAMETERS IN iTH-AREA OF LFC POWER SYSTEMS

Δf_i	frequency deviation
ΔP_{tie-i}	tie-line active power deviation
ΔP_{mi}	generator mechanical output deviation
ΔP_{vi}	valve position deviation
ΔP_{di}	load disturbance
M_i	moment of inertia of the genetator
D_i	damping coefficient of the genetator
T_{chi}	time constant of the turbine
T_{gi}	time constant of the governor
R_i	speed drop
β_i	frequency bias factor
T_{ij}	lie-line synchronizing coefficient between the ith and jth control area

$$\omega(t) = \left[\omega_1^{\mathrm{T}} \quad \dots \quad \omega_n^{\mathrm{T}}\right]^{\mathrm{T}},\ \bar{B} = \mathrm{diag}\left\{\bar{B}_1, \dots, \bar{B}_n\right\}$$
$$\bar{C} = \mathrm{diag}\left\{\bar{C}_1, \dots, \bar{C}_n\right\},\ \bar{E} = \mathrm{diag}\left\{\bar{E}_1, \dots, \bar{E}_n\right\}$$
$$\bar{C}_i = \left[\beta_i \quad 1 \quad 0 \quad 0\right],\ \bar{E}_i = \left[-\tfrac{1}{M_i} \quad 0 \quad 0 \quad 0\right]^{\mathrm{T}}$$
$$\bar{x}_i(t) = \left[\Delta f_i(t) \quad \Delta P_{\mathrm{tie}-i}(t) \quad \Delta P_{mi}(t) \quad \Delta P_{vi}(t)\right]^{\mathrm{T}}$$
$$\bar{y}_i(t) = \mathrm{ACE}_i(t),\ \omega_i(t) = \Delta P_{di}(t),\ \bar{A} = \left[\bar{A}_{ij}\right]_{n\times n}$$
$$\bar{A}_{ii} = \begin{bmatrix} -\frac{D_i}{M_i} & -\frac{1}{M_i} & \frac{1}{M_i} & 0 \\ 2\pi\sum_{j=1,j\neq i}^{n} T_{ij} & 0 & 0 & 0 \\ 0 & 0 & -\frac{1}{T_{chi}} & \frac{1}{T_{chi}} \\ -\frac{1}{R_i T_{gi}} & 0 & 0 & \frac{1}{T_{gi}} \end{bmatrix}$$
$$\bar{A}_{ij} = \begin{bmatrix} 0 & 0 & 0 & 0 \\ -2\pi T_{ij} & 0 & 0 & 0 \\ 0 & 0 & 0 & 0 \\ 0 & 0 & 0 & 0 \end{bmatrix},\ \bar{B}_i = \begin{bmatrix} 0 \\ 0 \\ 0 \\ \frac{1}{T_{gi}} \end{bmatrix}.$$

It should be noted that the ACE signal in the ith area is associated with not only the frequency deviation but also tie-line power exchange between areas, which is defined as follows:

$$\mathrm{ACE}_i(t) = \beta_i \Delta f_i(t) + \Delta P_{\mathrm{tie}-i}(t). \tag{2}$$

The purpose of this paper is to design the PI controller applied in the LFC power systems, which can be expressed as

$$u_i(t) = -K_{P_i}\mathrm{ACE}_i(t) - K_{I_i}\int_0^t \mathrm{ACE}_i(s)ds \tag{3}$$

where K_{P_i} and K_{I_i} denote the controller gains.

Define $y_i(t) = \left[\mathrm{ACE}_i(t) \quad \int_0^t \mathrm{ACE}_i(s)ds\right]^{\mathrm{T}}$ and $y(t) = \left[y_1^{\mathrm{T}}(t) \quad \dots \quad y_n^{\mathrm{T}}(t)\right]^{\mathrm{T}}$, then the control input of the multiarea LFC system can be rewritten as

$$u(t) = -Ky(t) \tag{4}$$

where $K = \mathrm{diag}\{K_1, K_2, \dots, K_n\}$ and $K_i = \left[K_{P_i} \quad K_{I_i}\right]$.

B. Event-Triggered Scheme Under DoS Attacks

In this section, to design a resilient LFC controller for multiarea power systems while reducing the amount of transmission in the network shown in Fig. 1, an event-triggered scheme will be put forward under the consideration of DoS attacks.

Define $x_i(t) = \left[\bar{x}_i^{\mathrm{T}}(t) \quad \int_0^t \mathrm{ACE}_i(s)ds\right]^{\mathrm{T}}$, then the measurement output of ith-area LFC system can be rewritten as

$$y_i(t) = C_i x_i(t) \tag{5}$$

where $C_i = \begin{bmatrix} \bar{C}_i & 0 \\ 0 & 1 \end{bmatrix}$. Furthermore, define $x(t) = \left[x_1^{\mathrm{T}}(t) \quad \dots \quad x_n^{\mathrm{T}}(t)\right]^{\mathrm{T}}$, $C = \mathrm{diag}\{C_1, \dots, C_n\}$, then for the multiarea LFC power system, the measurement output is

$$y(t) = Cx(t). \tag{6}$$

In this paper, the DoS attacks are assumed to be launched by a type of power-constraint periodic jamming signal [40], which is detectable and with the following representation:

$$\mathcal{T}_{\mathrm{DoS}}(t) = \begin{cases} 0, & t \in [(n-1)T, (n-1)T + T_{\mathrm{off}}) \\ 1, & t \in [(n-1)T + T_{\mathrm{off}}, nT) \end{cases} \tag{7}$$

where $n \in \mathbb{N}_{>0}$ is the period number, $T \in \mathbb{R}_{>0}$ denotes period of the jammer; T_{off} denotes the sleeping time of the jammer, which is lower bounded by $T_{\mathrm{off}}^{\min}$ in every period of jamming signal, namely, $T_{\mathrm{off}}^{\min} \leq T_{\mathrm{off}} < T$. Hence, within a period T, the interval $[0, T_{\mathrm{off}})$ denotes the sleeping interval of jamming signal and the interval $[T_{\mathrm{off}}, T)$ represents the active interval

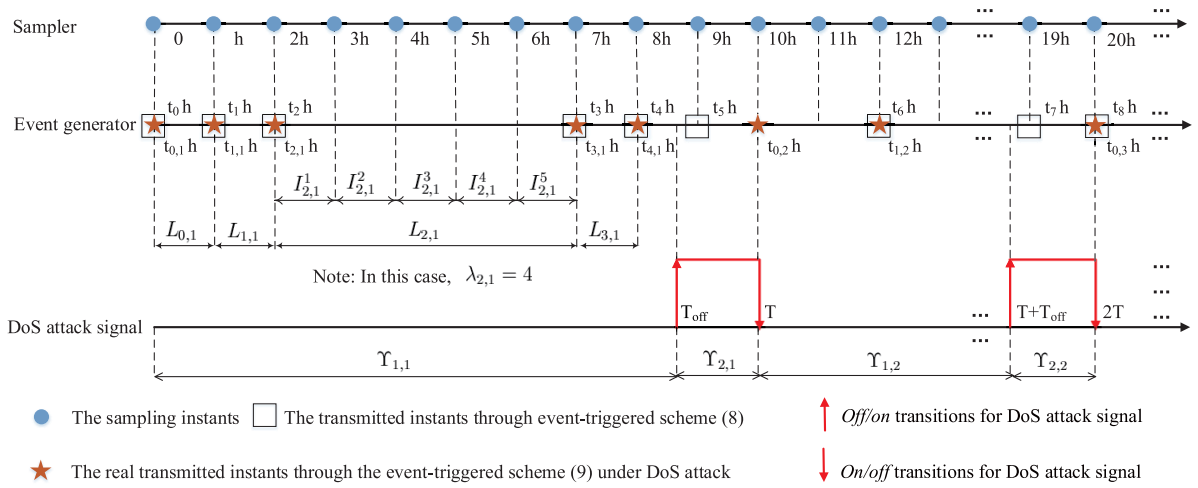

Fig. 2. Example of signal transmission through the event-triggered scheme under DoS attack.

of jamming signal. In other words, the communication is successful in every interval $[(n-1)T, (n-1)T + T_{\text{off}})$ while is denied in interval $[(n-1)T + T_{\text{off}}, nT)$.

Remark 1: How to model the DoS attacks is a basic issue when discussing the security problems in networked control areas. As stated in [15], there are various types of DoS attacks, such as trivial, periodic, random, and protocol-aware jamming attacks. Among the many different DoS attacks, the periodic or PWM DoS jamming signal with energy constraints [16] has been mostly investigated since it is much easier to handle benefiting from its characteristics such as detection avoidance and implementation simplicity. In this respect, to improve the feasibility when first dealing with the event-triggered H_∞ LFC problem for multiarea power systems under hybrid cyber attacks, we introduce the power-constraint periodic jamming signal (7) to model the DoS attacks in this paper. However, it is an interesting work to model the nonperiodic jamming signal, which will be considered in our future research.

In order to facilitate the development of event-triggered scheme under DoS attack signal (7), Assumption 1 is provided in the following, which is partially motivated by [16].

Assumption 1: The measurement outputs in all control area are assumed to be synchronously sampled in the same sampling period h ($h > 0$). Whether the sampled measurement to be transmitted over a network or not is determined by an event-triggered scheme. Under the event-triggered scheme, the transmission time sequence is assumed as $\{t_l h | t_l \in \mathbb{N}, l = 0, 1, 2, \ldots\}$. Time-delays, packet losses, and disorder are not discussed in this paper, which might be induced by the communication network.

In the absence of DoS jamming attacks, a common event-triggered condition [31] is given as

$$e^{\mathrm{T}}(t)\Phi e(t) \le \sigma x^{\mathrm{T}}(t_l h + jh) C^{\mathrm{T}} \Phi C x(t_l h + jh) \tag{8}$$

where $e(t) = y(t_l h) - y(t_l h + jh)$ ($j \in \mathbb{N}$) denotes the error, σ is a predefined scalar confined in the interval $[0, 1)$ and $\Phi = \text{diag}\{\Phi_1, \ldots, \Phi_n\} > 0$ is a weighting matrix to be determined later.

Remark 2: The event-triggered scheme depends on the deployment of event generator in each control area, where an event-triggered condition (8) is predefined. The operation mechanism is that if the event-triggered condition (8) is violated, the transmission event will be triggered; otherwise, the newly sampled data will be discarded directly.

Inspired by [40], when taking the DoS jamming attacks into consideration, the transmitted instants under event-triggered scheme (8) can be revised as

$$\begin{aligned} t_{l,n}h = \{&t_l h + jh \text{ satisfies } (8) | t_l h + jh \\ &\in [(n-1)T, (n-1)T + T_{\text{off}})\} \cup \{(n-1)T\} \end{aligned} \tag{9}$$

where $l+1$ represents the number of triggering times occurring in nth jammer period.

Remark 3: Compared with the event-triggered scheme (8) in the presence of normal transmission, it can be seen from (9) that the possible transmission events take place at the start of each period of DoS attack signal and the instants obeying the common event condition (8) as well as falling into the sleeping time of jamming signal. Moreover, compared with the event-triggered scheme in [40], this condition has no need to require that the jammer constantly maintains a "worst-case jamming scenario," which can be considered as an extension of [40].

Under the event-triggered scheme (9), the real transmitted packets are

$$y(t_{l,n}h) = Cx(t_{l,n}h) \tag{10}$$

where $l \in \{0, 1, \ldots, l(n)\}$ with $l(n) \triangleq \sup\{l \in \mathbb{N} | t_{l,n}h \le (n-1)T + T_{\text{off}}\}$. In particular, $t_{0,n}h \triangleq (n-1)T$, $(h < T)$. Fig. 2 depicts an example of signal transmission through the event-triggered scheme (9) under DoS attack, which might shed light on the following modeling process.

For notational simplicity, define

$$\begin{cases} r(n) \triangleq \{0, 1, \ldots, l(n)\} \\ \Upsilon_{1,n} \triangleq [(n-1)T, (n-1)T + T_{\text{off}}) \\ \Upsilon_{2,n} \triangleq [(n-1)T + T_{\text{off}}, nT) \\ L_{l,n} \triangleq \left[t_{l,n}h, t_{l+1,h}h\right), \ l \in r(n). \end{cases} \tag{11}$$

Notice these subintervals as follows:

$$L_{l,n} = \left\{\cup_{m=1}^{\lambda_{l,n}}\left[t_{l,n}h + (m-1)h, t_{l,n}h + mh\right)\right\} \cup \left[t_{l,n}h + \lambda_{l,n}h, t_{l+1,n}h\right) \tag{12}$$

where $l \in r(n)$, $n \in \mathbb{N}$, and $\lambda_{l,n} \triangleq \sup\{m \in \mathbb{N} | t_{l,n}h + mh < t_{l+1,n}h, m = 1, 2, \ldots\}$.

Let

$$\begin{cases} I_{l,n}^m = \left[t_{l,n}h + (m-1)h, t_{l,n}h + mh\right) \\ \qquad m \in \left\{1, 2, \ldots, \lambda_{l,n}\right\} \\ I_{l,n}^{\lambda_{l,n}+1} = \left[t_{l,n}h + \lambda_{l,n}h, t_{l+1,n}h\right). \end{cases} \tag{13}$$

Then, it can be deduced that

$$\Upsilon_{1,n} = \cup_{l=0}^{l(n)} \cup_{m=1}^{\lambda_{l,n}+1} \left\{I_{l,n}^m \cap \Upsilon_{1,n}\right\}. \tag{14}$$

Set

$$\phi_{l,n}^m = I_{l,n}^m \cap \Upsilon_{1,n} \tag{15}$$

then $\Upsilon_{1,n} = \cup_{l=0}^{l(n)} \cup_{m=1}^{\lambda_{l,n}+1} \phi_{l,n}^m$. For $l \in r(n)$, $n \in \mathbb{N}$, the following two piecewise functions are defined:

$$d_{l,n}(t) = \begin{cases} t - t_{l,n}h, & t \in \phi_{l,n}^1 \\ t - t_{l,n}h - h, & t \in \phi_{l,n}^2 \\ \qquad \vdots & \\ t - t_{l,n}h - \lambda_{l,n}h, & t \in \phi_{l,n}^{\lambda_{l,n}+1} \end{cases} \tag{16}$$

$$e_{l,n}(t) = \begin{cases} 0, & t \in \phi_{l,n}^1 \\ y\left(t_{l,n}h\right) - y\left(t_{l,n}h + h\right), & t \in \phi_{l,n}^2 \\ \qquad \vdots & \\ y\left(t_{l,n}h\right) - y\left(t_{l,n}h + \lambda_{l,n}h\right), & t \in \phi_{l,n}^{\lambda_{l,n}+1} \end{cases} \tag{17}$$

which mean $d_{l,n}(t) \in [0, h),\ t \in L_{l,n} \cap \Upsilon_{1,n},\ l \in r(n)$.

Combining (16) and (17), the real transmitted data (10) can be rewritten as

$$y\left(t_{l,n}h\right) = e_{l,n}(t) + Cx\left(t - d_{l,n}(t)\right) \quad t \in L_{l,n} \cap \Upsilon_{1,n},\ l \in r(n). \tag{18}$$

C. Deception Attacks

In this paper, deception attacks are also taken into consideration, which corrupt the transmission data by fully replacing the transmitted data with malicious attack signals. As it is assumed in [41] that the attackers have the ability to steal the transmitted data and disguise them with deceptive information. In this respect, the malicious signal can be modeled as a nonlinear function $g(y(t))$ [42]–[45], which is related to the transmitted data and is confined in Assumption 2.

Remark 4: Since the types of deception attacks contain an incorrect sensor measurement or control input, an incorrect time stamp, or a wrong identity of the sending device [46], there are different assumptions on the signals sent by deception attacks as long as they can achieve the deceptive goal. For example, in [46], the signal delivered by deception attacks are supposed to obey normal distribution. In this paper, a nonlinear function related to the measurable outputs is assumed to be modeled as the signal of deception attacks, which realizes the modification of the transmitted data and even destabilizes the multiarea power systems. Furthermore, inspired by [42]–[45], we restrict the nonlinear function with Assumption 2, which overcomes the mathematical challenge when analyzing this kind of deception attacks.

Note that the launching of deception attacks can be in consecutive or random fashion in order to achieve the attack goal [46]. In the following, it is further assumed that the deception attacks occur in a random manner, which is guaranteed by a Bernoulli random variable $\beta(t) \in \{0, 1\}$ with given statistical properties [47], i.e., expectation $\mathbb{E}\{\beta(t)\} = \bar{\beta}$ and variance $\mathbb{E}\{(\beta(t) - \bar{\beta})^2\} \triangleq \delta^2$. Then the real measurements arriving at controller are as follows:

$$\bar{y}(t) = \beta(t)g\left(y\left(t_{l,n}h\right)\right) + (1 - \beta(t))y\left(t_{l,n}h\right). \tag{19}$$

Remark 5: The Bernoulli random variable $\beta(t)$ in (19) can characterize the random occurring feature of deception attacks. To be more concrete, if $\beta(t) = 1$, (19) becomes $\bar{y}(t) = g(y(t_{l,n}h))$, which means that the deception attacks take place in the transmission process. If $\beta(t) = 0$, (19) changes into $\bar{y}(t) = y(t_{l,n}h)$, which indicates that the sampled measurements are successfully transmitted to feed controller.

D. New Switched System Model for Multiarea Power System

By considering event-triggered scheme under DoS attacks and deception attacks, the real control input of multiarea LFC systems is

$$u(t) = \begin{cases} -(1 - \beta(t))KCx\left(t - d_{l,n}(t)\right) \\ -(1 - \beta(t))Ke_{l,n}(t) \\ -\beta(t)Kg\left(y\left(d_{l,n}h\right)\right), & t \in L_{l,n} \cap \Upsilon_{1,n} \\ 0, & t \in \Upsilon_{2,n}. \end{cases} \tag{20}$$

Remark 6: In this paper, the input of controller (4), which arrives at the controller by the aid of open network, is subject to hybrid cyber attacks, namely DoS attacks and deception attacks. The real control input of multiarea LFC systems (20) is derived from (4) in view of the following reasons. If the DoS attacks take place, the process of data transmission is blocked, then $u(t) = 0$ for $t \in \Upsilon_{2,n}$; otherwise, the data transmission is normal while the deception attacks may randomly occur. Then, the update of control input is achievable, i.e., $u(t) = -K\bar{y}(t)$ for $t \in L_{l,n} \cap \Upsilon_{1,n}$.

Combining (1) and (20), the dynamic model of event-triggered H_∞ LFC multiarea power system under hybrid cyber

$$\begin{cases} \dot{x}(t) = \begin{cases} Ax(t) + E\omega(t) - \beta(t)BKg\left(y\left(t_{l,n}h\right)\right) - (1 - \beta(t))BK\left[e_{l,n}(t) + Cx\left(t - d_{l,n}(t)\right)\right], & t \in L_{l,n} \cap \Upsilon_{1,n} \\ Ax(t) + E\omega(t), & t \in \Upsilon_{2,n} \end{cases} \\ y(t) = Cx(t), \quad t \in \left(L_{l,n} \cap \Upsilon_{1,n}\right) \cup \Upsilon_{2,n}; \qquad x(t) = \psi(t), \quad t \in [-h, 0) \end{cases} \tag{21}$$

attacks can be expressed as (21), as shown at the bottom of the previous page, where

$$A = \left[A_{ij}\right]_{n\times n},\ A_{ii} = \begin{bmatrix}\bar{A}_{ii} & 0\\ \bar{C}_i & 0\end{bmatrix},\ A_{ij} = \begin{bmatrix}\bar{A}_{ij} & 0\\ 0 & 0\end{bmatrix}$$
$$B = \mathrm{diag}\{B_1,\ldots,B_n\},\ B_i = \begin{bmatrix}\bar{B}_i^{\mathrm{T}} & 0\end{bmatrix}^{\mathrm{T}}$$
$$E = \mathrm{diag}\{E_1,\ldots,E_n\},\ E_i = \begin{bmatrix}\bar{E}_i^{\mathrm{T}} & 0\end{bmatrix}^{\mathrm{T}}.$$

K and C is defined in (4) and (6), respectively. $e_{l,n}(t)$ satisfies the following constraint:

$$e_{l,n}^{\mathrm{T}}(t)\Phi e_{l,n}^{\mathrm{T}}(t) \le \sigma x^{\mathrm{T}}\big(t-d_{l,n}(t)\big)C^{\mathrm{T}}\Phi Cx\big(t-d_{l,n}(t)\big). \tag{22}$$

E. Problem of Interest

Before stating the problem to be addressed in this paper, we introduce the following assumption and definition.

Assumption 2 [42]–[45]: To restraint the deception attacks, the following condition of nonlinear function $g(y)$:

$$\|g(y)\|^2 \le \|Gy\|^2 \tag{23}$$

holds, where G is a constant matrix standing for the upper bound of the nonlinearity.

Definition 1 [48]: The zero solution of (21) is said to be exponentially stable in the mean-square sense if there exist two scalars $\tau > 0$ and $\varepsilon > 0$ such that $\mathbb{E}\{\|x(t)\|^2\} \le \tau\mathbb{E}\{\|\psi\|^2\}e^{-\varepsilon t}\ \forall t \ge 0$.

The purpose of this paper is to design the event-triggered load frequency controllers (4) for multiarea power system (21), such that, in the presence of DoS attacks (22) and deception attacks (23), the multiarea power system (21) is exponentially mean-square stable, and H_∞ performance constraint is satisfied. More specifically, the following requirements are satisfied.

1) The LFC multiarea power system (21) with $\omega(t) = 0$ is exponentially stable in the mean-square sense as it is defined in Definition 1.
2) Under the zero-initial condition, the inequality $\mathbb{E}\{\int_0^\infty \|y(s)\|^2 ds\} < \gamma^2\mathbb{E}\{\int_0^\infty \|\omega(s)\|^2 ds\}$ holds for all nonzero $\omega(t) \in \mathcal{L}_2[0,\infty)$ and prescribed scalar $\gamma > 0$.

To proceed with, three lemmas are introduced, which are helpful to derive our desired results.

Lemma 1 [49]: Consider a given matrix $R = R^{\mathrm{T}} > 0$. Then, for all continuously differentiable function $\dot{x}(t)$ in $[\underline{\tau},\overline{\tau}] \to \mathbb{R}^n$, the following inequality holds:

$$-\int_{\underline{\tau}}^{\overline{\tau}} \dot{x}^{\mathrm{T}}(s)R\dot{x}(s)ds \le -\frac{1}{\overline{\tau}-\underline{\tau}}\begin{bmatrix}\Pi_1\\ \Pi_2\end{bmatrix}^{\mathrm{T}}\begin{bmatrix}R & *\\ 0 & 3R\end{bmatrix}\begin{bmatrix}\Pi_1\\ \Pi_2\end{bmatrix} \tag{24}$$

where

$$\Pi_1 = x(\overline{\tau}) - x\big(\underline{\tau}\big)$$
$$\Pi_2 = x(\overline{\tau}) + x\big(\underline{\tau}\big) - \frac{2}{\overline{\tau}-\underline{\tau}}\int_{\underline{\tau}}^{\overline{\tau}} x(s)ds.$$

Lemma 2 [50]: Suppose that there exists a matrix $N \in \mathbb{R}^{n\times n}$ satisfying that $\begin{bmatrix}R & *\\ N & R\end{bmatrix} \ge 0$ for given symmetric positive definite matrices $R \in \mathbb{R}^{n\times n}$. Then, for any scalar $\theta \in (0,1)$, the following inequality holds:

$$\begin{bmatrix}\frac{1}{\theta}R & 0\\ 0 & \frac{1}{1-\theta}R\end{bmatrix} \ge \begin{bmatrix}R & *\\ N & R\end{bmatrix}. \tag{25}$$

Lemma 3 [51]: Suppose matrix $W \in \mathbb{R}^{n\times m}$ is full column rank, which has singular decomposition $W = UW_0V$, where U and V are orthogonal matrices and $W_0 \in \mathbb{R}^{n\times m}$ is a rectangular diagonal matrix with positive real numbers on the diagonal in decreasing order of magnitude. Assume $P \in \mathbb{R}^{n\times n}$ is a symmetric matrix, then there exists a matrix X such that $PW = WX$ if and only if P has the form with $P = U\begin{bmatrix}P_1 & 0\\ 0 & P_2\end{bmatrix}U^{\mathrm{T}}$, where $P_1 \in \mathbb{R}^{m\times m}$ and $P_2 \in \mathbb{R}^{(n-m)\times(n-m)}$.

III. Main Results

In this section, before starting to analyze the stability of system (21) with H_∞ performance and to design the load frequency controller (4), a lemma as well as its proof will be presented by introducing a variable

$$\eta(t) = \begin{cases}1, & t \in [-h,0] \cup \left(\cup_{n\in\mathbb{N}}\Upsilon_{1,n}\right)\\ 2, & t \in \cup_{n\in\mathbb{N}}\Upsilon_{2,n}.\end{cases} \tag{26}$$

Moreover, for $\eta(t) = i \in \{1,2\}$ and $n \in \mathbb{N}$, define

$$l_{i,n} = \begin{cases}(n-1)T, & i = 1\\ (n-1)T + T_{\mathrm{off}}, & i = 2.\end{cases} \tag{27}$$

Lemma 4: For given positive scalar $\bar{\beta} > 0$, trigger parameter σ, matrices G, K and a jamming signal $\mathcal{T}_{\mathrm{DoS}}(t)$, where parameters T and $T_{\mathrm{off}}^{\min}$ are known. Then, if for some known scalars $h > 0$, $\alpha_i > 0$ there exist matrices $P_i > 0$, $Q_i > 0$, $S_i > 0$, $Z_i > 0$ $(i = 1,2)$, $\Phi > 0$, and N_j, W_j $(j = 1,2,3,4)$ with appropriate dimensions such that

$$\Omega_i = \begin{bmatrix}\Omega_1^i & * & *\\ \Omega_2^i & \Omega_3^i & *\\ \Omega_2^i & 0 & \Omega_4^i\end{bmatrix} < 0,\ i = 1,\ 2 \tag{28}$$

$$\Theta_1 = \begin{bmatrix}S_1 & * & * & *\\ 0 & 3S_1 & * & *\\ N_1 & N_2 & S_1 & *\\ N_3 & N_4 & 0 & 3S_1\end{bmatrix} \ge 0 \tag{29}$$

$$\Theta_2 = \begin{bmatrix}S_2 & * & * & *\\ 0 & 3S_2 & * & *\\ W_1 & W_2 & S_2 & *\\ W_3 & W_4 & 0 & 3S_2\end{bmatrix} \ge 0 \tag{30}$$

where

$$\Omega_1^1 = \begin{bmatrix}\Gamma^1 + \frac{e^{-2\alpha_1 h}}{h}\Delta^1 & * & * & *\\ \Omega_{15} & -\Phi & * & *\\ \Omega_{16} & 0 & -\bar{\beta}I & *\\ \Omega_{18} & \sqrt{\bar{\beta}}G & 0 & -\bar{\beta}I\end{bmatrix}$$

$$\Gamma^1 = \begin{bmatrix}\Gamma_1^1 & * & * & * & * & *\\ \Gamma_2^1 & \sigma C^{\mathrm{T}}\Phi C & * & * & * & *\\ 0 & 0 & -e^{-2\alpha_1 h}Q_1 & * & * & *\\ 0 & 0 & 0 & 0 & * & *\\ 0 & 0 & 0 & 0 & 0 & *\\ 0 & 0 & 0 & 0 & 0 & 0\end{bmatrix}$$

$$\Omega_1^2 = \Gamma^2 + \frac{1}{h}\Delta^2$$

$$\Gamma^2 = \begin{bmatrix} \Gamma_1^2 & * & * & * & * & * \\ 0 & 0 & * & * & * & * \\ 0 & 0 & -e^{2\alpha_2 h}Q_2 & * & * & * \\ 0 & 0 & 0 & 0 & * & * \\ 0 & 0 & 0 & 0 & 0 & * \\ 0 & 0 & 0 & 0 & 0 & 0 \end{bmatrix}$$

$$\Gamma_1^1 = 2\alpha_1 P_1 + A^{\mathrm{T}}P_1 + P_1 A + Q_1$$
$$\Gamma_2^1 = -\big(1-\bar{\beta}\big)C^{\mathrm{T}}K^{\mathrm{T}}B^{\mathrm{T}}P_1$$
$$\Delta_1^1 = 6R_1 + 2N_2^{\mathrm{T}} + 2N_4^{\mathrm{T}}$$
$$\Delta_2^1 = -2N_2^{\mathrm{T}} + 2N_4^{\mathrm{T}},\ \ \Delta_3^1 = 2N_3 + 2N_4$$
$$\Delta_4^1 = 6R_1 - 2N_3 + 2N_4,\ \ \Delta_5^1 = -4N_4$$
$$\Delta_1^2 = 6R_2 + 2W_2^{\mathrm{T}} + 2W_4^{\mathrm{T}}$$
$$\Delta_2^2 = -2W_2^{\mathrm{T}} + 2W_4^{\mathrm{T}},\ \ \Delta_3^2 = 2W_3 + 2W_4$$
$$\Delta_4^2 = 6R_2 - 2W_3 + 2W_4,\ \ \Delta_5^2 = -4W_4$$
$$\Omega_{11} = -2S_1 - N_1 - N_2 - N_3 - N_4$$
$$\Omega_{12} = -8S_1 + \mathrm{sym}(N_1 - N_2 + N_3 - N_4)$$
$$\Omega_{13} = -4Z_1 + N_1 + N_2 - N_3 - N_4$$
$$\Omega_{14} = -2S_1 - N_1 + N_2 + N_3 - N_4$$
$$\Omega_{15} = \begin{bmatrix} -\big(1-\bar{\beta}\big)K^{\mathrm{T}}B^{\mathrm{T}}P_1 & 0 & 0 & 0 & 0 & 0 \end{bmatrix}$$
$$\Omega_{16} = \begin{bmatrix} -\bar{\beta}K^{\mathrm{T}}B^{\mathrm{T}}P_1 & 0 & 0 & 0 & 0 & 0 \end{bmatrix}$$
$$\Omega_{18} = \begin{bmatrix} 0 & \sqrt{\bar{\beta}}GC & 0 & 0 & 0 & 0 \end{bmatrix}$$
$$\Gamma_1^2 = -2\alpha_2 P_2 + A^{\mathrm{T}}P_2 + P_2 A + Q_2$$
$$\Omega_{21} = -2S_2 - W_1 - W_2 - W_3 - W_4$$
$$\Omega_{22} = -8S_2 + \mathrm{sym}(W_1 - W_2 + W_3 - W_4)$$
$$\Omega_{23} = -4Z_2 + W_1 + W_2 - W_3 - W_4$$
$$\Omega_{24} = -2S_2 - W_1 + W_2 + W_3 - W_4$$
$$\Omega_3^1 = \mathrm{diag}\Big\{-P_1 S_1^{-1}P_1, -P_1 S_1^{-1}P_1\Big\}$$
$$\Omega_4^1 = \mathrm{diag}\Big\{-P_1 Z_1^{-1}P_1, -P_1 Z_1^{-1}P_1\Big\}$$
$$\Omega_2^2 = \begin{bmatrix} \sqrt{h}P_2 A & 0 & 0 & 0 & 0 & 0 \end{bmatrix}$$
$$\Omega_3^2 = -P_2 S_2^{-1}P_2,\ \Omega_4^2 = -P_2 Z_2^{-1}P_2,\ \delta = \sqrt{\bar{\beta}(1-\bar{\beta})}.$$

$\Delta^i (i = 1, 2)$ and Ω_2^1 can refer to the box on top of the page. Then along the trajectories of the system (21), the following holds:

$$\mathbb{E}\big\{\dot{V}_i(t)\big\} \le e^{2(-1)^i \alpha_i (t - l_{i,n})}\mathbb{E}\{V_i(t)\} \quad t \in \big[l_{i,n}, l_{3-i,n+i-1}\big) \tag{31}$$

where the Lyapunov–Krasovskii functional candidate $V_i(t)(i = 1, 2)$ is defined in (43).

Proof: See Appendix A. ∎

Now, it is time to disclose the sufficient conditions guaranteeing the system (21) exponentially stable in the mean-square sense based on Lemma 4.

Theorem 1: For given a jamming signal $\mathcal{T}_{\mathrm{DoS}}(t)$ with known parameters T and $T_{\mathrm{off}}^{\min}$, controller gain matrix K, and constant matrix G. Then, if for some known scalars α_i, μ_i, σ, and $\bar{\beta}$, there exist matrices $P_i > 0$ $Q_i > 0$, $S_i > 0$, $Z_i > 0$, $\Phi > 0$ $(i = 1, 2)$, and N_j, W_j $(j = 1, 2, 3, 4)$ with appropriate dimensions such that the inequalities (28)–(30) and

$$P_1 \le \mu_2 P_2 \tag{32}$$
$$P_2 \le \mu_1 e^{2(\alpha_1+\alpha_2)h}P_1 \tag{33}$$
$$Q_i \le \mu_{3-i} Q_{3-i} \tag{34}$$
$$R_i \le \mu_{3-i} R_{3-i} \tag{35}$$
$$Z_i \le \mu_{3-i} Z_{3-i} \tag{36}$$
$$0 < \rho = 2\alpha_1 T_{\mathrm{off}}^{\min} - 2\alpha_2\Big(T - T_{\mathrm{off}}^{\min}\Big) - 2(\alpha_1+\alpha_2)h - \ln(\mu_1\mu_2) \tag{37}$$

hold. The multiarea power system (21) under hybrid cyber attacks is exponentially stable in the mean-square sense with decay rate $\varepsilon = (\rho/T)$.

Proof: See Appendix B. ∎

Theorem 1 presents the sufficient conditions, which guarantee the exponentially mean-square stability of the multiarea power system (21). Furthermore, inspired by the approach in [52], H_∞ performance of system (21) will be analyzed in Theorem 2.

Theorem 2: For given a jmming signal $\mathcal{T}_{\mathrm{DoS}}(t)$ with known parameters T and $T_{\mathrm{off}}^{\min}$, controller gain matrix K, and constant matrix G, the system (21) is exponentially mean-square stable with an H_∞ performance level γ, if for some known scalars α_i, μ_i, σ, $\bar{\beta}$, and h, there exist matrices $P_i > 0$ $Q_i > 0$, $S_i > 0$, $Z_i > 0$ $(i = 1, 2)$, $\Phi > 0$, and N_j, W_j $(j = 1, 2, 3, 4)$ with appropriate dimensions such that (29), (30), (32)–(37) and the following inequalities are satisfied:

$$\hat{\Omega}_i = \begin{bmatrix} \hat{\Omega}_1^i & * & * \\ \hat{\Omega}_2^i & \Omega_3^i & * \\ \hat{\Omega}_2^i & 0 & \Omega_4^i \end{bmatrix} < 0,\ \ i = 1,\ 2 \tag{38}$$

where

$$\hat{\Omega}_1^1 = \begin{bmatrix} \hat{\Gamma}^1 + \frac{e^{-2\alpha_1 h}}{h}\Delta^1 & * & * & * & * \\ \Omega_{15} & -\Phi & * & * & * \\ \Omega_{16} & 0 & -\bar{\beta}I & * & * \\ \Omega_{17} & 0 & 0 & -\gamma^2 I & * \\ \Omega_{18} & \sqrt{\bar{\beta}}G & 0 & 0 & -\bar{\beta}I \end{bmatrix}$$

$$\Gamma^1 = \begin{bmatrix} \hat{\Gamma}_1^1 & * & * & * & * & * \\ \Gamma_2^1 & \sigma C^{\mathrm{T}}\Phi C & * & * & * & * \\ 0 & 0 & -e^{-2\alpha_1 h}Q_1 & * & * & * \\ 0 & 0 & 0 & 0 & * & * \\ 0 & 0 & 0 & 0 & 0 & * \\ 0 & 0 & 0 & 0 & 0 & 0 \end{bmatrix}$$

$$\hat{\Gamma}_1^1 = 2\alpha_1 P_1 + A^{\mathrm{T}}P_1 + P_1 A + Q_1 + C^{\mathrm{T}}C$$
$$\Omega_{17} = \begin{bmatrix} F^{\mathrm{T}}P_1 & 0 & 0 & 0 & 0 & 0 \end{bmatrix}$$
$$\Omega_1^2 = \begin{bmatrix} \hat{\Gamma}^2 + \frac{1}{h}\Delta^2 & * \\ \Omega_{25} & -\gamma^2 I \end{bmatrix}$$

$$\hat{\Gamma}^2 = \begin{bmatrix} \hat{\Gamma}_1^2 & * & * & * & * & * \\ 0 & 0 & * & * & * & * \\ 0 & 0 & -e^{2\alpha_2 h}Q_2 & * & * & * \\ 0 & 0 & 0 & 0 & * & * \\ 0 & 0 & 0 & 0 & 0 & * \\ 0 & 0 & 0 & 0 & 0 & 0 \end{bmatrix}$$

$$\hat{\Gamma}_1^2 = -2\alpha_2 P_2 + A^{\mathrm{T}}P_2 + P_2 A + Q_2 + C^{\mathrm{T}}C$$
$$\Omega_{25} = \begin{bmatrix} F^{\mathrm{T}}P_2 & 0 & 0 & 0 & 0 & 0 \end{bmatrix}$$
$$\hat{\Omega}_2^2 = \begin{bmatrix} \sqrt{h}P_2 A & 0 & 0 & 0 & 0 & 0 & \sqrt{h}P_2 F \end{bmatrix}.$$

$$\Delta^i = \begin{bmatrix} -4R_i - 4Z_i & * & * & * & * & * \\ \Omega_{i1} & \Omega_{i2} & * & * & * & * \\ \Omega_{i3} & \Omega_{i4} & -4R_i - 4Z_i & * & * & * \\ 6Z_i & 0 & 6Z_i & -12Z_i & * & * \\ 6R_i & \Delta_1^i & \Delta_2^i & 0 & -12R_i & * \\ \Delta_3^i & \Delta_4^i & 6R_i & 0 & \Delta_5^i & -12R_i \end{bmatrix},\ i = 1, 2$$

$$\Omega_2^1 = \begin{bmatrix} \sqrt{h}P_1A & -(1-\bar{\beta})\sqrt{h}P_1BKC & 0 & 0 & 0 & 0 & -(1-\bar{\beta})\sqrt{h}P_1BK & -(1-\bar{\beta})\sqrt{h}P_1BK \\ 0 & \delta\sqrt{h}P_1BKC & 0 & 0 & 0 & 0 & -\delta\sqrt{h}P_1BK & -\delta\sqrt{h}P_1BK \end{bmatrix}$$

$$\hat{\Omega}_2^1 = \begin{bmatrix} \sqrt{h}P_1A & -(1-\bar{\beta})\sqrt{h}P_1BKC & 0 & 0 & 0 & 0 & -(1-\bar{\beta})\sqrt{h}P_1BK & -(1-\bar{\beta})\sqrt{h}P_1BK & \sqrt{h}P_1F \\ 0 & \delta\sqrt{h}P_1BKC & 0 & 0 & 0 & 0 & -\delta\sqrt{h}P_1BK & -\delta\sqrt{h}P_1BK & 0 \end{bmatrix}$$

$$\tilde{\Omega}_2^1 = \begin{bmatrix} \sqrt{h}P_1A & -(1-\bar{\beta})\sqrt{h}BYC & 0 & 0 & 0 & 0 & -(1-\bar{\beta})\sqrt{h}BY & -(1-\bar{\beta})\sqrt{h}BY & \sqrt{h}P_1F \\ 0 & \delta\sqrt{h}BYC & 0 & 0 & 0 & 0 & -\delta\sqrt{h}BY & -\delta\sqrt{h}BY & 0 \end{bmatrix}$$

$\hat{\Omega}_2^1$ can refer to the box on top of this page. Other symbols are defined in Lemma 4.

Proof: See Appendix C. ∎

Remark 7: Theorem 2 proves H_∞ performance of the multiarea power system (21), which is motivated by [17] and [52]. In particular, the idea of proving H_∞ performance in [52] is adopted in this paper when solving the H_∞ LFC problem for multiarea power system (21).

The purpose of Theorem 3 is to design the H_∞ controller for system (21), where B is assumed to be full column rank and its singular value decomposition is represented by $B = U\begin{bmatrix} B_0^{\mathrm{T}} & 0 \end{bmatrix}^{\mathrm{T}} V$.

Theorem 3: For given a jamming signal $\mathcal{T}_{\mathrm{DoS}}(t)$ with known parameters T and $T_{\mathrm{off}}^{\min}$, constant matrix G, the system (21) is exponentially mean-square stable with an H_∞ performance level γ, if for some known scalars α_i, μ_i, σ, $\bar{\beta}$, h, ϵ_j $(j = 1, 2, 3, 4)$ there exist matrices $P_i > 0$ $Q_i > 0$, $S_i > 0$, $Z_i > 0$ $(i = 1, 2)$, $\Phi > 0$, Y and N_j, W_j $(j = 1, 2, 3, 4)$ with appropriate dimensions such that (29), (30), (32)–(37) and the following LMIs are satisfied:

$$\tilde{\Omega}_i = \begin{bmatrix} \tilde{\Omega}_1^i & * & * \\ \tilde{\Omega}_2^i & \tilde{\Omega}_3^i & * \\ \tilde{\Omega}_2^i & 0 & \tilde{\Omega}_4^i \end{bmatrix} < 0,\ i = 1,\ 2 \tag{39}$$

where

$$\tilde{\Omega}_1^1 = \begin{bmatrix} \tilde{\Gamma}^1 + \frac{e^{-2\alpha_1 h}}{h}\Delta^1 & * & * & * & * \\ \tilde{\Omega}_{15} & -\Phi & * & * & * \\ \tilde{\Omega}_{16} & 0 & -\bar{\beta}I & * & * \\ \Omega_{17} & 0 & 0 & -\gamma^2 I & * \\ \Omega_{18} & \sqrt{\bar{\beta}}G & 0 & 0 & -\bar{\beta}I \end{bmatrix}$$

$$\tilde{\Gamma}^1 = \begin{bmatrix} \Gamma_1^1 & * & * & * & * & * \\ \tilde{\Gamma}_2^1 & \sigma C^{\mathrm{T}}\Phi C & * & * & * & * \\ 0 & 0 & -e^{-2\alpha_1 h}Q_1 & * & * & * \\ 0 & 0 & 0 & 0 & * & * \\ 0 & 0 & 0 & 0 & 0 & * \\ 0 & 0 & 0 & 0 & 0 & 0 \end{bmatrix}$$

$$\tilde{\Gamma}_2^1 = -(1-\bar{\beta})C^{\mathrm{T}}Y^{\mathrm{T}}B^{\mathrm{T}},\ \tilde{\Omega}_1^2 = \Omega_1^2,\ \tilde{\Omega}_2^2 = \Omega_2^2$$

$$\tilde{\Omega}_{15} = \begin{bmatrix} -(1-\bar{\beta})Y^{\mathrm{T}}B^{\mathrm{T}} & 0 & 0 & 0 & 0 & 0 \end{bmatrix}$$

$$\tilde{\Omega}_{16} = \begin{bmatrix} -\bar{\beta}Y^{\mathrm{T}}B^{\mathrm{T}} & 0 & 0 & 0 & 0 & 0 \end{bmatrix}$$

$$\tilde{\Omega}_3^1 = \mathrm{diag}\left\{-2\epsilon_1 P_1 + \epsilon_1^2 R_1, -2\epsilon_1 P_1 + \epsilon_1^2 R_1\right\}$$

$$\tilde{\Omega}_4^1 = \mathrm{diag}\left\{-2\epsilon_2 P_1 + \epsilon_2^2 Z_1, -2\epsilon_2 P_1 + \epsilon_2^2 Z_1\right\}$$

$$\tilde{\Omega}_3^2 = -2\epsilon_3 P_2 + \epsilon_3^2 R_2,\ \tilde{\Omega}_4^2 = -2\epsilon_4 P_2 + \epsilon_4^2 Z_2.$$

$\tilde{\Omega}_2^1$ can refer to the box on top of this page. Other symbols are defined in Lemma 4. It should be pointed that $P_1 = U\begin{bmatrix} P_{11} & 0 \\ 0 & P_{12} \end{bmatrix}U^{\mathrm{T}}$ with $P_{11} \in \mathbb{R}^{m\times m}$ and $P_{12} \in \mathbb{R}^{(n-m)\times(n-m)}$. Moreover, the control gain matrix can be obtained

$$K = \left(B^{\mathrm{T}}P_1B\right)^{-1}B^{\mathrm{T}}BY. \tag{40}$$

Proof: See Appendix D. ∎

IV. Simulation Example

In this section, a simulation example related to a three-area power system is given to illustrate the usefulness of the proposed approach in designing event-triggered H_∞ load frequency controller subject to hybrid cyber attacks.

The system parameters of the three-area power system (1) are listed in Table II. Suppose that the sleeping time of the jammer T_{off} is constrained by $T = 1$ s and $T_{\mathrm{off}}^{\min} = 0.8$ s, namely, $0.8 \le T_{\mathrm{off}} \le 1$. Select $\mu_1 = \mu_2 = 1.01$, $\alpha_1 = 0.5$, $\alpha_2 = 0.35$, $h = 0.02$ s, $\epsilon_i = 1$, $(i = 1, 2, 3, 4)$, $\sigma = 0.4$, and H_∞ performance index $\gamma = 2$. Furthermore, we assume that the occurring expectation and nonlinear function of deception attacks are respectively, $\bar{\beta} = 0.05$ and $g(y(t)) = \begin{bmatrix} -\tanh(G_1y_1(t)) & -\tanh(G_2y_2(t)) & -\tanh(G_3y_3(t)) \end{bmatrix}^{\mathrm{T}}$, where $G_1 = \mathrm{diag}\{0.1, 0.1\}$, $G_2 = \mathrm{diag}\{0.25, 0.25\}$, and $G_3 = \mathrm{diag}\{0.05, 0.05\}$. Then, the condition (23) can be satisfied when specifying nonlinearity bound as $G = \mathrm{diag}\{G_1, G_2, G_3\}$.

In light of Theorem 3, the weighting matrix in event-trigger condition (22) is obtained as

$$\Phi = \mathrm{diag}\{\Phi_1, \Phi_2, \Phi_3\} \tag{41}$$

where

$$\Phi_1 = \begin{bmatrix} 5.1643 & 4.0768 \\ 4.0768 & 547.2205 \end{bmatrix},\ \Phi_2 = \begin{bmatrix} 4.7892 & 3.1717 \\ 3.1717 & 548.9645 \end{bmatrix}$$

TABLE II
PARAMETERS OF THE THREE-AREA LFC POWER SYSTEMS

Paremeters	$T_{ch}(s)$	$T_g(s)$	R	D	β	$M(s)$
Area1	0.3	0.1	0.05	1.0	21.0	10
Area2	0.4	0.17	0.05	1.5	21.5	12
Area3	0.35	0.20	0.05	1.8	21.8	12
$T_{12} = 0.1986$, $T_{13} = 0.2148$, $T_{23} = 0.1830$						

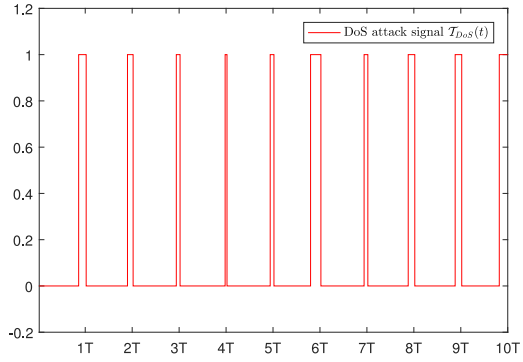

Fig. 3. DoS attack signal $\mathcal{T}_{\text{DoS}}(t)$ with $T = 1$ and 0.8 s $< T_{\text{off}} < 1$ s.

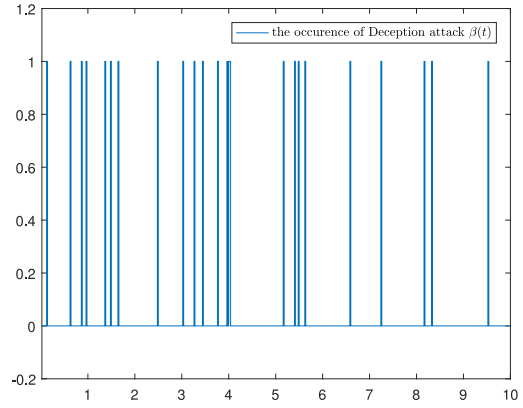

Fig. 4. $\beta(t)$ of deception attacks with $\bar{\beta} = 0.05$.

$$\Phi_3 = \begin{bmatrix} 4.7048 & 2.7447 \\ 2.7447 & 546.5687 \end{bmatrix}.$$

Moreover, the controller gain (4) can be figured out from (40) as

$$K = \text{diag}\{K_1, K_2, K_3\} \tag{42}$$

where

$$K_1 = \begin{bmatrix} -0.0571 & -0.0109 \end{bmatrix},\ K_2 = \begin{bmatrix} -0.0567 & -0.0108 \end{bmatrix}$$
$$K_3 = \begin{bmatrix} -0.0585 & -0.0107 \end{bmatrix}.$$

In particular, assume the disturbance $\omega(t)$ as follows:

$$\omega(t) = \begin{cases} \begin{bmatrix} \frac{\sin(0.125t)}{0.01t+0.01} \\ \frac{2.5\sin(0.25t)}{0.2t+0.1} \\ \frac{5\sin(0.1t)}{0.05t+0.01} \end{bmatrix}, & 0 \le t \le 8 \\ 0, & \text{otherwise} \end{cases}$$

and given the initial state as

$$\psi(t) = \begin{bmatrix} \psi_1^{\text{T}}(t) & \psi_2^{\text{T}}(t) & \psi_3^{\text{T}}(t) \end{bmatrix}^{\text{T}}$$

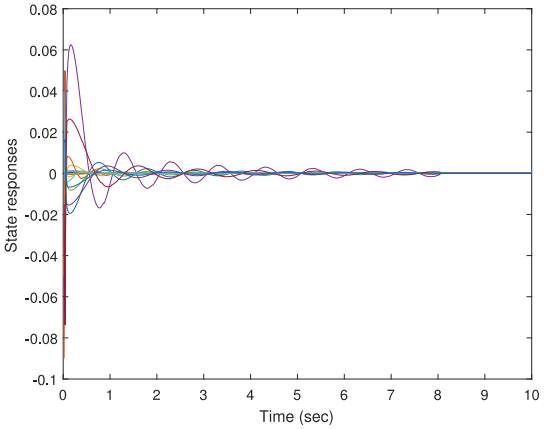

Fig. 5. State responses of the three-area power system under hybrid cyber attacks.

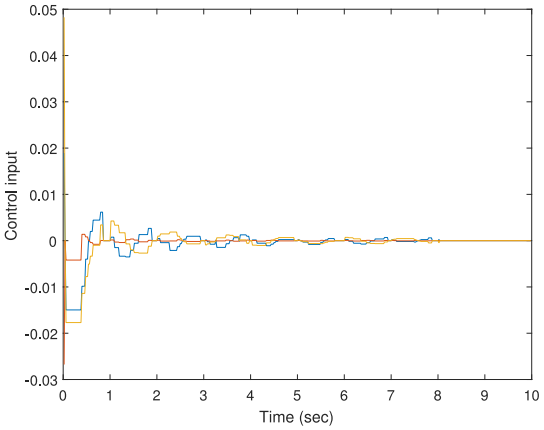

Fig. 6. Control input of the three-area power system under hybrid cyber attacks.

where

$$\psi_1(t) = \begin{bmatrix} 0.02 & -0.09 & 0.04 & -0.05 & 0.008 \end{bmatrix}^{\text{T}}$$
$$\psi_2(t) = \begin{bmatrix} -0.02 & -0.04 & 0.05 & -0.05 & -0.01 \end{bmatrix}^{\text{T}}$$
$$\psi_3(t) = \begin{bmatrix} 0.04 & -0.05 & 0.04 & -0.015 & 0.015 \end{bmatrix}^{\text{T}}$$

the following simulation results can be depicted. The signal of DoS attack with period $T = 1$ s and $T_{\text{off}}^{\min} = 0.8$ s is depicted in Fig. 3, where the value of T_{off} is confined in the interval $[0.8, 1)$. The Bernoulli variable $\beta(t)$ indicating the occurrence of deception attacks are characterized in Fig. 4 with $\bar{\beta} = 0.05$. Fig. 5 draws the state responses of the multiarea power system (21). The control input of three areas are presented in Fig. 6. The release time instants and intervals according to the event-triggered scheme under DoS attacks are shown in Fig. 7. In addition, $\|y(t)\| = 2.1336$ and $\|\omega(t)\| = 50.8242$ can be obtained by calculation, which deduce that $(\|y(t)\|/\|\omega(t)\|) = 0.0420 < \gamma$ ($\gamma = 2$). Thereby, the proposed approach in designing H_∞ load frequency controller (4) is effective. From the above simulation results for $t \in [0, 10$ s$]$, it can be concluded that the network transmission times are decreased and the stability of system (21) is guaranteed under the hybrid cyber attacks.

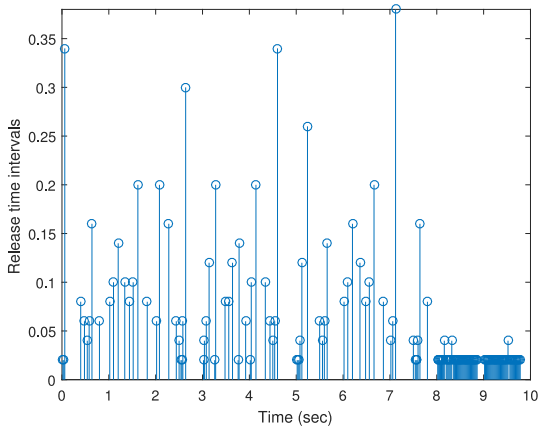

Fig. 7. Release time intervals under hybrid cyber attacks with $\bar{\beta} = 0.05$ and $0.8\ \text{s} < T_{\text{off}} < 1\ \text{s}$.

V. Conclusion

In this paper, the event-triggered H_∞ LFC problem has been investigated for the multiarea power systems under hybrid cyber attacks. By considering the effect of DoS attacks, an event-triggered scheme has been exploited to cut down the number of data transmission. Moreover, the sufficient conditions for exponentially mean-square stability with an H_∞ performance have been derived from a new switched system model, which integrates the characteristics of LFC multiarea power system, the event-triggered scheme under DoS attacks and stochastic deception attacks. In this case, the controller gain and the weighting matrix in event-triggered scheme have been obtained simultaneously, which are expressed in the form of LMIs. The simulation with respect to a three-area power system has verified the usefulness of the H_∞ load frequency controller designed in this paper.

Appendix A
Proof of Lemma 4

Choose a Lyapunov–Krasovskii functional candidate for system (21)

$$\begin{aligned} V_{\eta(t)}(t) &= x^{\mathrm{T}}(t)P_{\eta(t)}x(t) \\ &\quad + \int_{t-h}^{t} x^{\mathrm{T}}(s)\exp(\cdot)Q_{\eta(t)}x(s)ds \\ &\quad + \int_{-h}^{0}\int_{t+\nu}^{t} \dot{x}^{\mathrm{T}}(s)\exp(\cdot)S_{\eta(t)}\dot{x}(s)dsd\nu \\ &\quad + \int_{-h}^{0}\int_{t+\nu}^{t} \dot{x}^{\mathrm{T}}(s)\exp(\cdot)Z_{\eta(t)}\dot{x}(s)dsd\nu \end{aligned} \tag{43}$$

where $P_{\eta(t)} > 0$, $Q_{\eta(t)} > 0$, $S_{\eta(t)} > 0$, $Z_{\eta(t)} > 0$, $\alpha_{\eta(t)} > 0$, $\exp(\cdot) \triangleq e^{2(-1)^{\eta(t)}\alpha_{\eta(t)}(t-s)}$, and

$$\eta(t) = \begin{cases} 1, & t \in [-h, 0] \cup \left(\cup_{n\in\mathbb{N}} \Upsilon_{1,n}\right) \\ 2, & t \in \cup_{n\in\mathbb{N}} \Upsilon_{2,n}. \end{cases} \tag{44}$$

By taking derivation and expectation on $V_1(t)$ for $t \in L_{l,n} \cap \Upsilon_{1,n}$, it can be obtained that

$$\begin{aligned} \mathbb{E}\{\dot{V}_1(t)\} &\le -2\alpha_1 V_1(t) + 2\alpha_1 x^{\mathrm{T}}(t)P_1x(t) \\ &\quad + 2\mathbb{E}\{x^{\mathrm{T}}(t)P_1\dot{x}(t)\} + x^{\mathrm{T}}(t)Q_1x(t) \\ &\quad - x^{\mathrm{T}}(t-h)e^{-2\alpha_1 h}Q_1x(t-h) \\ &\quad + \mathbb{E}\{h\dot{x}^{\mathrm{T}}(t)(S_1+Z_1)\dot{x}(t)\} \\ &\quad - \int_{t-h}^{t} \dot{x}^{\mathrm{T}}(s)e^{-2\alpha_1 h}Z_1\dot{x}(t)ds \\ &\quad - \int_{t-h}^{t} \dot{x}^{\mathrm{T}}(s)e^{-2\alpha_1 h}S_1\dot{x}(t)ds. \end{aligned} \tag{45}$$

Define $\xi(t) = [x(t), x(t-d_{l,n}(t)), x(t-h), (1/h)\int_{t-h}^{t} x(s)ds, (1/[d_{l,n}(t)])\int_{t-d_{l,n}(t)}^{t} x(s)ds, [1/(h-d_{l,n}(t))]\int_{t-h}^{t-d_{l,n}(t)} x(s)ds]^{\mathrm{T}}$, By applying Lemma 1, the following inequalities can be obtained:

$$\begin{aligned} &-\int_{t-h}^{t} \dot{x}^{\mathrm{T}}(s)e^{-2\alpha_1 h}Z_1\dot{x}(s)ds \\ &\quad \le -\frac{e^{-2\alpha_1 h}}{h}\begin{bmatrix}\Pi_1\\ \Pi_2\end{bmatrix}^{\mathrm{T}}\begin{bmatrix}Z_1 & * \\ 0 & 3Z_1\end{bmatrix}\begin{bmatrix}\Pi_1\\ \Pi_2\end{bmatrix} \end{aligned} \tag{46}$$

$$\begin{aligned} &-\int_{t-d_{l,n}(t)}^{t} \dot{x}^{\mathrm{T}}(s)e^{-2\alpha_1 h}S_1\dot{x}(s)ds \\ &\quad \le -\frac{e^{-2\alpha_1 h}}{d_{l,n}(t)}\hat{\Pi}_1^{\mathrm{T}}\hat{S}_1\hat{\Pi}_1 \end{aligned} \tag{47}$$

$$\begin{aligned} &-\int_{t-h}^{t-d_{l,n}(t)} \dot{x}^{\mathrm{T}}(s)e^{-2\alpha_1 h}S_1\dot{x}(s)ds \\ &\quad \le -\frac{e^{-2\alpha_1 h}}{h-d_{l,n}(t)}\hat{\Pi}_2^{\mathrm{T}}\hat{S}_1\hat{\Pi}_2 \end{aligned} \tag{48}$$

where

$$\begin{aligned} &\Pi_1 = (e_1 - e_3)\xi(t),\ \ \Pi_2 = (e_1 + e_3 - 2e_4)\xi(t) \\ &\Pi_3 = (e_1 - e_2)\xi(t),\ \ \Pi_4 = (e_1 + e_2 - 2e_5)\xi(t) \\ &\Pi_5 = (e_2 - e_3)\xi(t),\ \ \Pi_6 = (e_2 + e_3 - 2e_6)\xi(t) \\ &\hat{\Pi}_1 = \begin{bmatrix}\Pi_3\\ \Pi_4\end{bmatrix},\ \hat{S}_1 = \begin{bmatrix}S_1 & * \\ 0 & 3S_1\end{bmatrix},\ \hat{\Pi}_2 = \begin{bmatrix}\Pi_5\\ \Pi_6\end{bmatrix} \end{aligned}$$

$e_i (i = 1, 2, 3, 4, 5, 6)$ are compatible row-block matrices with ith block of an identify matrix.

Combining (47) and (48) and adopting Lemma 2, it can be derived that

$$\begin{aligned} &-\int_{t-h}^{t} \dot{x}^{\mathrm{T}}(s)e^{-2\alpha_1 h}R_1\dot{x}(s)ds \\ &\quad \le -\frac{e^{-2\alpha_1 h}}{h}\begin{bmatrix}\hat{\Pi}_1\\ \hat{\Pi}_2\end{bmatrix}\begin{bmatrix}\frac{h}{d_{l,n}(t)}\hat{S}_1 & * \\ 0 & \frac{h}{h-d_{l,n}(t)}\hat{S}_1\end{bmatrix}\begin{bmatrix}\hat{\Pi}_1\\ \hat{\Pi}_2\end{bmatrix} \\ &\quad \le -\frac{e^{-2\alpha_1 h}}{h}\begin{bmatrix}\hat{\Pi}_1\\ \hat{\Pi}_2\end{bmatrix}^{\mathrm{T}}\begin{bmatrix}\hat{S}_1 & * \\ \hat{N} & \hat{S}_1\end{bmatrix}\begin{bmatrix}\hat{\Pi}_1\\ \hat{\Pi}_2\end{bmatrix} \end{aligned} \tag{49}$$

when $\begin{bmatrix}\hat{S}_1 & * \\ \hat{N} & \hat{S}_1\end{bmatrix} \ge 0$ where $\hat{N} = \begin{bmatrix}N_1 & N_2 \\ N_3 & N_4\end{bmatrix}$.

Recalling the assumption of deception attacks (23), the following inequality condition can be obtained:

$$\bar{\beta}y^{\mathrm{T}}(t_{l,n}h)G^{\mathrm{T}}Gy(t_{l,n}h) - \bar{\beta}g^{\mathrm{T}}(y(t_{l,n}h))g(y(t_{l,n}h)) \ge 0 \tag{50}$$

where $y(t_{l,n}h)$ satisfies (10).

Furthermore, define $\xi_1(t) = [\xi^{\mathrm{T}}(t), e_{l,n}(t), g(y(t_{l,n}))]^{\mathrm{T}}$ and $e_i (i = 7, 8)$ are compatible row-block matrices with ith block of an identify matrix. Then $2\mathbb{E}\{x^{\mathrm{T}}(t)P_1\dot{x}(t)\} = 2x^{\mathrm{T}}(t)P_1[\mathcal{A}_0 + \mathcal{A}_1]\xi_1(t)$, where $\mathcal{A}_0 = Ae_1$ and $\mathcal{A}_1 = -\bar{\beta}BKe_8 - (1-\bar{\beta})BKe_7 - (1-\bar{\beta})BKCe_2$ since the random variable $\mathbb{E}\{\beta(t)\} = \bar{\beta}$.

Besides, $\dot{x}(t) = \left[\mathcal{B}_0 + (\beta(t) - \bar{\beta})\mathcal{B}_1\right]\xi_1(t)$, where $\mathcal{B}_0 = \mathcal{A}_0 - \bar{\beta}BKe_8 - (1-\bar{\beta})BKe_7 + (1-\bar{\beta})BKCe_2$ and $\mathcal{B}_1 = -BKe_8 + BKe_7 + BKCe_2$. Moreover, $\mathbb{E}\{\beta(t) - \bar{\beta}\} = 0$ and $\mathbb{E}(\beta(t) - \bar{\beta})^2 = \delta^2$. Therefore

$$\mathbb{E}\left\{h\dot{x}^{\mathrm{T}}(t)(S_1 + Z_1)\dot{x}(t)\right\} = \xi_1^{\mathrm{T}}(t)\mathcal{B}_0^{\mathrm{T}}h(S_1 + Z_1)\mathcal{B}_0\xi_1(t) + \delta^2\xi_1^{\mathrm{T}}(t)\mathcal{B}_1^{\mathrm{T}}h(S_1 + Z_1)\mathcal{B}_1\xi_1(t). \tag{51}$$

Then, combining (45)–(51), it can be obtained that

$$\mathbb{E}\left\{\dot{V}_1(t)\right\} \le -2\alpha_1\mathbb{E}\{V_1(t)\} + \xi_1^{\mathrm{T}}(t) \times \left[\Omega_1^1 + \mathcal{B}_0^{\mathrm{T}}h(S_1 + Z_1)\mathcal{B}_0 + \delta^2\mathcal{B}_1^{\mathrm{T}}h(S_1 + Z_1)\mathcal{B}_1\right]\xi_1(t). \tag{52}$$

By using Schur complement, $\Omega_1 < 0$ and $\Theta_1 \ge 0$ means that $\mathbb{E}\{\dot{V}_1(t)\} \le -2\alpha_1\mathbb{E}\{V_1(t)\}$ holds.

In addition, define $\xi_2(t) = \xi(t)$. By taking derivation and expectation on $V_2(t)$ for $t \in \Upsilon_{2,n}$, it can be obtained that

$$\mathbb{E}\left\{\dot{V}_2(t)\right\} \le 2\alpha_2\mathbb{E}\{V_2(t)\} + \xi_2^{\mathrm{T}}(t) \times \left[\Omega_1^2 + \mathcal{A}_0^{\mathrm{T}}h(S_2 + Z_2)\mathcal{A}_0\right]\xi_2(t). \tag{53}$$

Similarly, $\Omega_2 < 0$ and $\Theta_2 \ge 0$ indicate $\mathbb{E}\{\dot{V}_2(t)\} \le 2\alpha_2\mathbb{E}\{V_2(t)\}$.

This completes the proof.

Appendix B
Proof of Theorem 1

Construct a time-varying Lyapunov functional as in the proof of Lemma 4: $V(t) = V_{\eta(t)}(t)$ and $\eta(t) \in \{1, 2\}$. From Lemma 4, one has

$$\mathbb{E}\{V(t)\} \le \begin{cases} e^{-2\alpha_1(t-l_{1,n})}\mathbb{E}\left\{V_1\left(l_{1,n}\right)\right\}, & t \in \left[l_{1,n}, l_{2,n}\right) \\ e^{2\alpha_2(t-l_{2,n})}\mathbb{E}\left\{V_2\left(l_{2,n}\right)\right\}, & t \in \left[l_{2,n}, l_{1,n+1}\right). \end{cases} \tag{54}$$

From (32)–(37), it can be obtained that

$$\begin{cases} \mathbb{E}\left\{V_1\left(l_{1,n}\right)\right\} \le \mu_2\mathbb{E}\left\{V_2\left(l_{1,n}^-\right)\right\} \\ \mathbb{E}\left\{V_2\left(l_{2,n}\right)\right\} \le \mu_1 e^{2(\alpha_1+\alpha_2)h}\mathbb{E}\left\{V_1\left(l_{2,n}^-\right)\right\}. \end{cases} \tag{55}$$

If $t \in [l_{1,n}, l_{2,n})$, it follows from (54) and (55) that:

$$\mathbb{E}\{V(t)\} \le \mu_2 e^{-2\alpha_1(t-l_{1,n})}\mathbb{E}\left\{V_2\left(l_{1,n}^-\right)\right\} \le (\mu_1\mu_2)^n e^{q+2(\alpha_1+\alpha_2)n}\mathbb{E}\left\{V_1\left(l_{1,0}\right)\right\} \tag{56}$$

where $q = -2\alpha_1[(t - l_{1,n}) + (l_{2,n-1} - l_{1,n-1}) + \cdots + (l_{1,0} - l_{2,0})] + 2\alpha_2[(l_{1,n} - l_{2,n-1}) + (l_{1,n-1} - l_{2,n-2}) + \cdots + (l_{1,1} - l_{2,0})]$. Notice that it follows from the definition of DoS jamming signals (7) that $q < -2\alpha_1 nT_{\mathrm{off}}^{\min} + 2\alpha_2 n(T - T_{\mathrm{off}}^{\min})$ since $T_{\mathrm{off}}^{\min} \le T_{\mathrm{off}} < T$. Therefore

$$\mathbb{E}\{V(t)\} \le e^{-\rho n}V_1(0). \tag{57}$$

In particular, $[(t - T_{\mathrm{off}}^{\min})/T] < n \le (t/T)$ can be derived from $nT = l_{1,n} \le t \le l_{2,n} = nT + T_{\mathrm{off}}^{\min}$. Hence,

$$\mathbb{E}\{V(t)\} \le V_1(0)e^{\frac{\rho T_{\mathrm{off}}^{\min}}{T}}e^{-\frac{\rho}{T}t}, \ t \in \left[l_{1,n}, l_{2,n}\right). \tag{58}$$

Similarly, it can be deduced that

$$\mathbb{E}\{V(t)\} \le \frac{V_1(0)}{\mu_2}e^{-\frac{\rho}{T}t}, \ t \in \left[l_{2,n}, l_{1,n+1}\right). \tag{59}$$

On one hand, define $c = \max\{e^{(\rho T_{\mathrm{off}}^{\min}/T)}, (1/\mu_2)\}$, $c_1 = \min\{\lambda_{\min}(P_i)\}$, $c_2 = \max\{\lambda_{\max}(P_i)\}$, $c_3 = c_2 + h\lambda_{\max}(Q_1) + (h^2/2)\lambda_{\max}(S_1 + Z_1)$, and $\varepsilon = (\rho/T)$, from (58) and (59), it achieves that

$$\mathbb{E}\{V(t)\} \le ce^{-\frac{\rho}{T}t}\mathbb{E}\{V_1(0)\} \ \ \forall t \ge 0. \tag{60}$$

On the other hand, it can be derived from the definition of $V(t)$ that

$$\mathbb{E}\{V(t)\} \ge c_1\mathbb{E}\left\{\|x(t)\|^2\right\}, \ \mathbb{E}\{V_1(0)\} \le c_3\mathbb{E}\left\{\|\psi\|^2\right\}. \tag{61}$$

Therefore, it follows from (60) and (61) that:

$$\mathbb{E}\left\{\|x(t)\|^2\right\} \le \frac{cc_3}{c_1}e^{-\varepsilon t}\mathbb{E}\left\{\|\psi\|^2\right\} \ \ \forall t \ge 0 \tag{62}$$

which proves that the system (21) is exponentially stable in the mean-square sense with decay rate ε.

This completes the proof.

Appendix C
Proof of Theorem 2

By the similar proof adopted in Lemma 4 based on the time-varying Lyapunov functional (43), it can be deduced that for $t \in \Upsilon_{1,n}$

$$\mathbb{E}\left\{\dot{V}_1(t)\right\} \le -2\alpha_1\mathbb{E}\{V_1(t)\} + \hat{\xi}_1^{\mathrm{T}}(t)\Big[\hat{\Omega}_1^1 + \hat{\mathcal{B}}_0^{\mathrm{T}}h(S_1 + Z_1)\hat{\mathcal{B}}_0 + \delta^2\mathcal{B}_1^{\mathrm{T}}h(S_1 + Z_1)\mathcal{B}_1\Big]\hat{\xi}_1(t) - \mathbb{E}\left\{y^{\mathrm{T}}(t)y(t)\right\} + \gamma^2\mathbb{E}\left\{\omega^{\mathrm{T}}(t)\omega(t)\right\} \tag{63}$$

where $\hat{\xi}_1(t) = [\xi_1^{\mathrm{T}}(t), \omega(t)]^{\mathrm{T}}$, $\hat{\mathcal{B}}_0 = \hat{\mathcal{A}}_0 - \bar{\beta}BKe_8 - (1 - \bar{\beta})BKe_7 + (1 - \bar{\beta})BKCe_2$, and $\hat{\mathcal{A}}_0 = Ae_1 + Ee_9$.

By using Schur complement, (63) is written as

$$\mathbb{E}\left\{\dot{V}_1(t)\right\} + 2\alpha_1\mathbb{E}\{V_1(t)\} + \mathbb{E}\left\{y^{\mathrm{T}}(t)y(t)\right\} - \gamma^2\mathbb{E}\left\{\omega^{\mathrm{T}}(t)\omega(t)\right\} \le \hat{\xi}_1^{\mathrm{T}}(t)\hat{\Omega}_1\hat{\xi}_1(t). \tag{64}$$

Then, from (38) and (64), it follows that:

$$\mathbb{E}\left\{\dot{V}_i(t)\right\} + 2(-1)^{i+1}\alpha_i\mathbb{E}\{V_i(t)\} + \mathbb{E}\left\{y^{\mathrm{T}}(t)y(t)\right\} - \gamma^2\mathbb{E}\left\{\omega^{\mathrm{T}}(t)\omega(t)\right\} \le 0, \ t \in \left[l_{i,n}, l_{3-i,n+i-1}\right). \tag{65}$$

Notice that for all $\omega(t) \in \mathcal{L}_2[0, \infty)$ in $t \in [0, (n+1)T)$, (66) as shown at the top of the next page, can be deduced from (54) and (55) by referring to the proof in [52].

Moreover, it can be deduced from inequality (37) and the constraint $T_{\mathrm{off}}^{\min} \le T_{\mathrm{off}} < T$ that

$$\frac{1}{\mu_1}e^{2\alpha_1 T_{\mathrm{off}} - 2(\alpha_1+\alpha_2)h} - \mu_2 e^{2\alpha_2(T - T_{\mathrm{off}})} > 0. \tag{67}$$

$$\sum_{m=0}^{n}\left(\int_{mT}^{mT+T_{\text{off}}}\mathbb{E}\big[\dot{V}_1(t)+2\alpha_1 V_1(t)\big]dt+\int_{mT+T_{\text{off}}}^{(m+1)T}\mathbb{E}\big[\dot{V}_2(t)-2\alpha_2 V_2(t)\big]dt\right)$$
$$\geq -V_1(0)+\sum_{m=0}^{n-1}\left(\frac{1}{\mu_1}e^{2\alpha_1 T_{\text{off}}-2(\alpha_1+\alpha_2)h}-\mu_2 e^{2\alpha_2(T-T_{\text{off}})}\right)\mathbb{E}\{V_2(mT+T_{\text{off}})\}$$
$$+\left(\frac{1}{\mu_1}e^{2\alpha_1 T_{\text{off}}-2(\alpha_1+\alpha_2)h}-\mu_2 e^{2\alpha_2(T-T_{\text{off}})}\right)\mathbb{E}\{V_2(nT+T_{\text{off}})\}+\mathbb{E}\{V_2((n+1)T+T_{\text{off}})\} \quad (66)$$

Then, under the zero-initial condition, further combine (66) and (67), it derives that

$$\sum_{m=0}^{n}\left(\int_{mT}^{mT+T_{\text{off}}}\mathbb{E}\big[\dot{V}_1(t)+2\alpha_1 V_1(t)\big]dt+\int_{mT+T_{\text{off}}}^{(m+1)T}\mathbb{E}\big[\dot{V}_2(t)-2\alpha_2 V_2(t)\big]dt\right)>0. \quad (68)$$

Therefore, by integrating both sides of (65) from 0 to $(n+1)T$, it follows from (68) that:

$$\int_0^{(n+1)T}\Big(\mathbb{E}\big\{y^{\mathrm{T}}(t)y(t)\big\}-\gamma^2\mathbb{E}\big\{\omega^{\mathrm{T}}(t)\omega(t)\big\}\Big)dt<0. \quad (69)$$

Let $t\to\infty$, it yields from (69) that

$$\mathbb{E}\left\{\int_0^{\infty}y^{\mathrm{T}}(t)y(t)dt\right\}\leq\gamma^2\mathbb{E}\left\{\int_0^{\infty}\omega^{\mathrm{T}}(t)\omega(t)dt\right\} \quad (70)$$

for all $\omega(t)\in\mathcal{L}_2[0,+\infty)$ with zero-initial condition.

This completes the proof.

Appendix D
Proof of Theorem 3

It is easy to obtain that

$$\Big(S_1-\epsilon_1^{-1}P_1\Big)S_1^{-1}\Big(S_1-\epsilon_1^{-1}P_1\Big)\geq 0 \quad (71)$$

since $S_1\geq 0$. Then by simple calculations, it follows that:

$$-P_1S_1^{-1}P_1\leq -2\epsilon_1P_1+\epsilon_1^2S_1. \quad (72)$$

Accordingly,

$$\begin{cases}-P_1Z_1^{-1}P_1\leq -2\epsilon_2P_1+\epsilon_2^2Z_1\\ -P_2S_2^{-1}P_2\leq -2\epsilon_3P_2+\epsilon_3^2S_2\\ -P_2Z_2^{-1}P_2\leq -2\epsilon_4P_2+\epsilon_4^2Z_2.\end{cases} \quad (73)$$

Therefore, $\tilde{\Omega}_3^1$, $\tilde{\Omega}_4^1$, $\tilde{\Omega}_3^2$, and $\tilde{\Omega}_4^2$ are derived from Ω_3^1, Ω_4^1, Ω_3^2, and Ω_4^2 by applying (72) and (73), respectively.

In addition, notice that $P_1=U\begin{bmatrix}P_{11}&0\\0&P_{12}\end{bmatrix}U^{\mathrm{T}}$ and $B=U\begin{bmatrix}B_0^{\mathrm{T}}&0\end{bmatrix}^{\mathrm{T}}V$. Then from Lemma 3, there exits a $m\times m$ matrix X such that $P_1B=BX$. Further more, define $Y=XK$, it follows that $P_1BK=BXK=BY$. By replacing P_1BK in Theorem 2 with BY, Theorem 3 is obtained. Moreover, the control gain matrix is designed as $K=(B^{\mathrm{T}}P_1B)^{-1}B^{\mathrm{T}}BY$ by referring to the proof in [51].

This completes the proof.

References

[1] S. Liu, W. Luo, and L. Wu, "Co-design of distributed model-based control and event-triggering scheme for load frequency regulation in smart grids," *IEEE Trans. Syst., Man, Cybern., Syst.*, to be published. doi: 10.1109/TSMC.2018.2866965.

[2] F. Liu, Y. Li, Y. Cao, J. She, and M. Wu, "A two-layer active disturbance rejection controller design for load frequency control of interconnected power system," *IEEE Trans. Power Syst.*, vol. 31, no. 4, pp. 3320–3321, Jul. 2016.

[3] S. D. Hanwate, Y. V. Hote, and S. Saxena, "Adaptive policy for load frequency control," *IEEE Trans. Power Syst.*, vol. 33, no. 1, pp. 1142–1144, Jan. 2018.

[4] S. Liu and P. X. Liu, "Distributed model-based control and scheduling for load frequency regulation of smart grids over limited bandwidth networks," *IEEE Trans. Ind. Informat.*, vol. 14, no. 5, pp. 1814–1823, May 2018.

[5] L. Dong, Y. Tang, H. He, and C. Sun, "An event-triggered approach for load frequency control with supplementary ADP," *IEEE Trans. Power Syst.*, vol. 32, no. 1, pp. 581–589, Jan. 2017.

[6] L. Jiang, W. Yao, Q. H. Wu, J. Y. Wen, and S. Cheng, "Delay-dependent stability for load frequency control with constant and time-varying delays," *IEEE Trans. Power Syst.*, vol. 27, no. 2, pp. 932–941, May 2012.

[7] C. Peng and J. Zhang, "Delay-distribution-dependent load frequency control of power systems with probabilistic interval delays," *IEEE Trans. Power Syst.*, vol. 31, no. 4, pp. 3309–3317, Jul. 2016.

[8] Z. H. Fang, H. D. Mo, and Y. Wang, "Reliability analysis of cyber-physical systems considering cyber-attacks," in *Proc. IEEE IEEM*, Singapore, 2017, pp. 364–368.

[9] H. Yuan and Y. Xia, "Secure filtering for stochastic non-linear systems under multiple missing measurements and deception attacks," *IET Control Theory Appl.*, vol. 12, no. 4, pp. 515–523, Mar. 2018.

[10] D. Ding, Z. Wang, Q.-L. Han, and G. Wei, "Security control for discrete-time stochastic nonlinear systems subject to deception attacks," *IEEE Trans. Syst., Man, Cybern., Syst.*, vol. 48, no. 5, pp. 779–789, May 2018.

[11] Y. Li, L. Shi, and T. Chen, "Detection against linear deception attacks on multi-sensor remote state estimation," *IEEE Trans. Control Netw. Syst.*, vol. 5, no. 3, pp. 846–856, Sep. 2018.

[12] Y. Guan and X. Ge, "Distributed attack detection and secure estimation of networked cyber-physical systems against false data injection attacks and jamming attacks," *IEEE Trans. Signal Inf. Process. Netw.*, vol. 4, no. 1, pp. 48–59, Mar. 2018.

[13] G. K. Befekadu, V. Gupta, and P. J. Antsaklis, "Risk-sensitive control under Markov modulated denial-of-service (DoS) attack strategies," *IEEE Trans. Autom. Control*, vol. 60, no. 12, pp. 3299–3304, Dec. 2015.

[14] C. Peng, J. Li, and M. Fei, "Resilient event-triggering H_∞ load frequency control for multi-area power systems with energy-limited DoS attacks," *IEEE Trans. Power Syst.*, vol. 32, no. 5, pp. 4110–4118, Sep. 2017.

[15] C. D. Persis and P. Tesi, "Input-to-state stabilizing control under denial-of-service," *IEEE Trans. Autom. Control*, vol. 60, no. 11, pp. 2930–2944, Nov. 2015.

[16] S. Hu, D. Yue, X. Xie, X. Chen, and X. Yin, "Resilient event-triggered controller synthesis of networked control systems under periodic DoS jamming attacks," *IEEE Trans. Cybern.*, to be published. doi: 10.1109/TCYB.2018.2861834.

[17] J. Liu, T. Yin, M. Shen, X. Xie, and J. Cao, "State estimation for cyber–physical systems with limited communication resources, sensor saturation and denial-of-service attacks," *ISA Trans.*, Dec. 2018, doi: 10.1016/j.isatra.2018.12.032.

[18] L. Zha, E. Tian, X. Xie, Z. Gu, and J. Cao, "Decentralized event-triggered H_∞ control for neural networks subject to cyber-attacks," *Inf. Sci.*, vols. 457–458, pp. 141–155, Aug. 2018.

[19] E. Mousavinejad, F. Yang, Q.-L. Han, and L. Vlacic, "A novel cyber attack detection method in networked control systems," *IEEE Trans. Cybern.*, vol. 48, no. 11, pp. 3254–3264, Nov. 2018.

[20] D. Ding, Q.-L. Han, Y. Xiang, X. Ge, and X.-M. Zhang, "A survey on security control and attack detection for industrial cyber-physical systems," *Neurocomputing*, vol. 275, pp. 1674–1683, Jan. 2018.

[21] B. Chen, D. W. C. Ho, W.-A. Zhang, and L. Yu, "Distributed dimensionality reduction fusion estimation for cyber-physical systems under DoS attacks," *IEEE Trans. Syst., Man, Cybern., Syst.*, vol. 49, no. 2, pp. 455–468, Feb. 2019.

[22] D. Ding, Z. Wang, Q.-L. Han, and G. Wei, "Neural-network-based output-feedback control under round-Robin scheduling protocols," *IEEE Trans. Cybern.*, to be published. doi: 10.1109/TCYB.2018.2827037.

[23] X. Xie, Q. Zhou, D. Yue, and H. Li, "Relaxed control design of discrete-time Takagi–Sugeno fuzzy systems: An event-triggered real-time scheduling approach," *IEEE Trans. Syst., Man, Cybern., Syst.*, vol. 48, no. 12, pp. 2251–2262, Dec. 2018.

[24] X.-M. Zhang, Q.-L. Han, and X. Yu, "Survey on recent advances in networked control systems," *IEEE Trans. Ind. Informat.*, vol. 12, no. 5, pp. 1740–1752, Oct. 2016.

[25] X. Ge, Q.-L. Han, and Z. Wang, "A dynamic event-triggered transmission scheme for distributed set-membership estimation over wireless sensor networks," *IEEE Trans. Cybern.*, vol. 49, no. 1, pp. 171–183, Jan. 2019.

[26] Z.-G. Wu, Y. Xu, R. Lu, Y. Wu, and T. Huang, "Event-triggered control for consensus of multiagent systems with fixed/switching topologies," *IEEE Trans. Syst., Man, Cybern., Syst.*, vol. 48, no. 10, pp. 1736–1746, Oct. 2018.

[27] D. Yao, B. Zhang, P. Li, and H. Li, "Event-triggered sliding mode control of discrete-time Markov jump systems," *IEEE Trans. Syst., Man, Cybern., Syst.*, to be published. doi: 10.1109/TSMC.2018.2836390.

[28] X. Ge and Q.-L. Han, "Distributed formation control of networked multi-agent systems using a dynamic event-triggered communication mechanism," *IEEE Trans. Ind. Electron.*, vol. 64, no. 10, pp. 8118–8127, Oct. 2017.

[29] C. Peng, Q.-L. Han, and D. Yue, "To transmit or not to transmit: A discrete event-triggered communication scheme for networked Takagi–Sugeno fuzzy systems," *IEEE Trans. Fuzzy Syst.*, vol. 21, no. 1, pp. 164–170, Feb. 2013.

[30] X. Ge, F. Yang, and Q.-L. Han, "Distributed networked control systems: A brief overview," *Inf. Sci.*, vol. 380, pp. 117–131, Feb. 2017.

[31] D. Yue, E. Tian, and Q.-L. Han, "A delay system method for designing event-triggered controllers of networked control systems," *IEEE Trans. Autom. Control*, vol. 58, no. 2, pp. 475–481, Feb. 2013.

[32] X.-M. Zhang and Q.-L. Han, "Event-triggered dynamic output feedback control for networked control systems," *IET Control Theory Appl.*, vol. 8, no. 4, pp. 226–234, Mar. 2014.

[33] C. Peng, D. Yue, and M.-R. Fei, "A higher energy-efficient sampling scheme for networked control systems over IEEE 802.15.4 wireless networks," *IEEE Trans. Ind. Informat.*, vol. 12, no. 5, pp. 1766–1774, Oct. 2016.

[34] C. Peng, J. Zhang, and Q.-L. Han, "Consensus of multiagent systems with nonlinear dynamics using an integrated sampled-data-based event-triggered communication scheme," *IEEE Trans. Syst., Man, Cybern., Syst.*, vol. 49, no. 3, pp. 589–599, Mar. 2019. doi: 10.1109/TSMC.2018.2814572.

[35] J. Liu, Z. Wu, D. Yue, and J. H. Park, "Stabilization of networked control systems with hybrid-driven mechanism and probabilistic cyber attacks," *IEEE Trans. Syst., Man, Cybern., Syst.*, to be published. doi: 10.1109/TSMC.2018.2888633.

[36] J. Liu, L. Wei, J. Cao, and S. Fei, "Hybrid-driven H_∞ filter design for T–S fuzzy systems with quantization," *Nonlin. Anal. Hybrid Syst.*, vol. 31, pp. 135–152, Feb. 2019.

[37] X.-M. Zhang, Q.-L. Han, and B.-L. Zhang, "An overview and deep investigation on sampled-data-based event-triggered control and filtering for networked systems," *IEEE Trans. Ind. Informat.*, vol. 13, no. 1, pp. 4–16, Feb. 2017.

[38] L. Ding, Q.-L. Han, X. Ge, and X.-M. Zhang, "An overview of recent advances in event-triggered consensus of multiagent systems," *IEEE Trans. Cybern.*, vol. 48, no. 4, pp. 1110–1123, Apr. 2018.

[39] X. Ge, Q.-L. Han, D. Ding, X.-M. Zhang, and B. Ning, "A survey on recent advances in distributed sampled-data cooperative control of multi-agent systems," *Neurocomputing*, vol. 275, pp. 1684–1701, Jan. 2018.

[40] X. Chen, Y. Wang, and S. Hu, "Event-based robust stabilization of uncertain networked control systems under quantization and denial-of-service attacks," *Inf. Sci.*, vol. 459, pp. 369–386, Aug. 2018.

[41] L. An and G.-H. Yang, "Improved adaptive resilient control against sensor and actuator attacks," *Inf. Sci.*, vol. 423, pp. 145–156, Jan. 2018.

[42] J. Liu, Y. Gu, X. Xie, D. Yue, and J. H. Park, "Hybrid-driven-based H_∞ control for networked cascade control systems with actuator saturations and stochastic cyber attacks," *IEEE Trans. Syst., Man, Cybern., Syst.*, to be published. doi: 10.1109/TSMC.2018.2875484.

[43] J. Liu, E. Tian, X. Xie, and L. Hong, "Distributed event-triggered control for networked control systems with stochastic cyber-attacks," *J. Frankl. Inst.*, Mar. 2018, doi: 10.1016/j.jfranklin.2018.01.048.

[44] J. Liu, L. Wei, X. Xie, and D. Yue, "Distributed event-triggered state estimators design for sensor networked systems with deception attacks," *IET Control Theory Appl.*, to be published. doi: 10.1049/iet-cta.2018.5868.

[45] J. Liu, L. Wei, X. Xie, E. Tian, and S. Fei, "Quantized stabilization for T–S fuzzy systems with hybrid-triggered mechanism and stochastic cyber-attacks," *IEEE Trans. Fuzzy Syst.*, vol. 26, no. 6, pp. 3820–3834, Dec. 2018.

[46] D. Ding, G. Wei, S. Zhang, Y. Liu, and F. E. Alsaadi, "On scheduling of deception attacks for discrete-time networked systems equipped with attack detectors," *Neurocomputing*, vol. 219, pp. 99–106, Jan. 2017.

[47] E. Tian, W. K. Wong, D. Yue, and T.-C. Yang, "H_∞ filtering for discrete-time switched systems with known sojourn probabilities," *IEEE Trans. Autom. Control*, vol. 60, no. 9, pp. 2446–2451, Sep. 2015.

[48] J. P. Hespanha, P. Naghshtabrizi, and Y. Xu, "A survey of recent results in networked control systems," *Proc. IEEE*, vol. 95, no. 1, pp. 138–162, Jan. 2007.

[49] A. Seuret and F. Gouaisbaut, "Wirtinger-based integral inequality: Application to time-delay systems," *Automatica*, vol. 49, no. 9, pp. 2860–2866, 2013.

[50] P. Park, J. W. Ko, and C. Jeong, "Reciprocally convex approach to stability of systems with time-varying delays," *Automatica*, vol. 47, no. 1, pp. 235–238, 2011.

[51] Q.-L. Han, Y. Liu, and F. Yang, "Optimal communication network-based H_∞ quantized control with packet dropouts for a class of discrete-time neural networks with distributed time delay," *IEEE Trans. Neural Netw. Learn. Syst.*, vol. 27, no. 2, pp. 426–434, Feb. 2016.

[52] S. Hu, Y. Zhou, X. Chen, and Y. Ma, "H_∞ controller design of event-triggered networked control systems under quantization and denial-of-service attacks," in *Proc. 37th Chin. Control Conf.*, Wuhan, China, 2018, pp. 6338–6343.

Jinliang Liu received the Ph.D. degree in control theory and control engineering from Donghua University, Shanghai, China, in 2011.

He was a Post-Doctoral Research Associate with Southeast University, Nanjing, China, from 2013 to 2016. From 2016 to 2017, he was a Visiting Researcher/Scholar with the University of Hong Kong, Hong Kong. From 2017 to 2018, he was a Visiting Scholar with Yeungnam University, Gyeongsan, South Korea. He is currently an Associate Professor with the Nanjing University of Finance and Economics, Nanjing. His current research interests include networked control systems, complex dynamical systems, and T–S fuzzy systems.

Yuanyuan Gu was born in Jiangsu, China, in 1994. She received the B.S. degree in medical information from Xuzhou Medical University, Xuzhou, China, in 2016. She is currently pursuing the M.S. degree with the College of Information Engineering, Nanjing University of Finance and Economics, Nanjing, China.

Her current research interests include networked control systems, power systems, and time delay systems.

Lijuan Zha received the Ph.D. degree in control theory and control engineering from Donghua University, Shanghai, China, in 2018.

She is currently a Lecturer with the Nanjing University of Finance and Economics, Nanjing, China, and has been a Post-Doctoral Research Associate with the School of Mathematics, Southeast University, Nanjing, since 2018. Her current research interests include networked control systems, neural networks, and complex dynamical systems.

Yajuan Liu received the B.S. degree in mathematics and applied mathematics from Shanxi Normal University, Linfen, China, in 2010, the M.S. degree in applied mathematics from the University of Science and Technology Beijing, Beijing, China, in 2012, and the Ph.D. degree from the Division of Electronic Engineering, Daegu University, Deagu, South Korea, in 2015.

Since 2015, she has been a Post-Doctoral Research Fellow with the Department of Electrical Engineering, Yeungnam University, Gyeongsan. She is currently a Lecturer with the North China Electric Power University, Beijing, China. Her current research interest includes control of dynamic systems, including neural networks and complex systems.

Jie Cao received the Ph.D. degree in control theory and control engineering from Southeast University, Nanjing, China, in 2002.

He is currently a Professor and the Dean of the School of Information Engineering, Nanjing University of Finance and Economics, Nanjing. He has been selected in the Program for New Century Excellent Talents in University and awarded with Young and Mid-Aged Expert with Outstanding Contribution in Jiangsu Province. His current research interests include social network analysis and complex systems.